Spring 2018

Development of Electronic Testing Devices That Detect Peripheral Neuropathies

Peter Svendsen
University of New Hampshire, Durham

DEVELOPMENT OF ELECTRONIC TESTING DEVICES THAT DETECT PERIPHERAL NEUROPATHIES

BY

Peter J. Svendsen
B.S., Computer Engineering, University of New Hampshire, 2015

THESIS

Submitted to the University of New Hampshire
in partial fulfillment of
the requirements for the degree of

Master of Science
in
Electrical Engineering

May 2018

This thesis has been examined and approved in partial fulfillment of the degrees of Master of Science in Electrical Engineering by:

Thesis Director, Dr. John R. LaCourse
Professor
Department of Electrical and Computer Engineering

Dr. Wayne J. Smith
Senior Lecturer
Department of Electrical and Computer Engineering

Dr. Ron Croce
Professor
Department of Kinesiology

On April 20th, 2018

Original approval signatures are on file with the University of New Hampshire Graduate School.

DEDICATION

For my family:

Mom Dad

Kristen Mike Jon Yuhui Jen Shane Justin Keith

Christian Ginny Lilac

Aaron Danny Willow

Amelia Stephanie

Kate

Lindsey

ACKNOWLEDGMENTS

I would like to thank Dr. LaCourse, Dr. Smith and Dr. Croce for all the help they have given me over the course of this research.

I would also like to thank my sister Kristen for helping me proofread this paper.

TABLE OF CONTENTS

LIST OF FIGURES

LIST OF TABLES

LIST OF EQUATIONS

ABSTRACT

DEVELOPMENT OF ELECTRONIC TESTING DEVICES THAT DETECT PERIPHERAL NEUROPATHIES

by

Peter J. Svendsen

University of New Hampshire, May 2018

There are a number of different testing devices to detect carpal tunnel syndrome and other peripheral neuropathies. Electronic tests known as nerve conduction studies assess the health of a nerve by measuring the amplitude and velocity of action potentials traveling along that nerve. The action potentials are generated by stimulating the nerve with a high voltage. The shape, duration and amplitude of the high voltage stimulus are all carefully selected in order to make the stimulus both safe and effective. Nerve conduction studies are generally considered reliable and accurate. However, they are very complex and expensive.

Over the course of this research, a stimulus device and two simple electronic devices to detect peripheral neuropathies were developed and tested. The stimulus device was used by both testing devices to generate nerve action potentials. The first device recorded the nerve action potentials so they could be used to assess nerve health. The second device assessed nerve health by measuring the motor response of a digit to stimulation. In the end, neither of the two testing devices was successfully used to assess nerve health. However, an effective stimulus device was developed. This device was able to stimulate motor responses in both the median and ulnar nerves.

1. INTRODUCTION

1.1 Nerve Conduction

Testing the functionality of a nerve is a key part of diagnosing peripheral nerve disorders such as Carpal Tunnel Syndrome. Nerve conduction studies are advanced electronic tests that are commonly used to assess nerve health [1]. Nerve conduction studies measure the velocity and amplitude of an electrical impulse traveling along a nerve. The electrical impulse is generated by attaching electrodes near a nerve and stimulating the nerve with a high voltage. The electrical impulse generated by the nerve is known as an action potential. An action potential can be observed and recorded at other locations along the same nerve. Nerves that are damaged or diseased do not transmit electrical energy effectively and have less than ideal action potentials [2]. Nerve conduction studies are a reliable way of confirming a diagnosis of Carpal Tunnel Syndrome [2].

1.2 Carpal Tunnel Syndrome

Carpal tunnel syndrome is a peripheral nervous disorder that affects the median nerve [3]. It is the most common entrapment neuropathy [4]. It is caused by the compression of the median nerve as it passes through the carpal tunnel [5]. The symptoms of the disorder include numbness, tingling and hand pain [3]. Carpal tunnel syndrome may also cause the muscles of the thumb to weaken [5]. A survey of 2,466 Swedish people found that 14.4% had experienced numbness, tingling and hand pain [6]. After performing nerve conduction studies and clinical examinations, researchers estimated that one in five of the symptomatic people had Carpal Tunnel Syndrome [6].

1.3 Alternative Devices

Nerve conduction study devices, while effective at detecting peripheral neuropathies, are expensive, painful and time-consuming [7]. Several portable electronic devices exist to diagnose peripheral neuropathies such as the Neurosentinal, Nervepace Electroneurometer, and Brevio. The Neurosentinal stimulates a nerve and then measures the time it takes the sensory nerve signal to travel to another location [8]. The nerve must be stimulated four times and produce similar latency times for the results to be considered valid [8]. The travel time of the sensory nerve signal is used to assess the health of the nerve. The Nervepace Electroneurometer stimulates a motor nerve and then measures the time delay before muscle contractions to occur [8]. The time delay before the muscle to contract is used to assess the health of the nerve. The Electroneurometer can average the results of multiple tests together to get more percise results [8]. The Brevio is a newer portable device for measuring nerve conduction velocity partly based on the Nervepace Electroneurometer [9]. Studies evaluating the effectiveness of this specific device were not found. All these portable devices have limitations when compared to full nerve conduction study devices. However, the existence of these devices show that it is possible for simpler electronic devices to detect peripheral neuropathies.

1.4 Thesis Contributions

The main goal of this research was to develop a simple electronic device that accurately assessed nerve health. Two devices to assess nerve health were developed and tested over the course of this research. Both these devices required a stimulus device, which had to be developed and tested as well.

The first device designed was a simple nerve conduction study apparatus. This device was supposed to record action potentials traveling along the nerve axon. The recorded action potentials would then be used to assess nerve health. Nerve health assessment would be based on the conduction velocity and amplitude of the action potentials. However, this device was never actually able to record action potentials. This device was validated by testing it on a human. In order to protect the test subject from electrical shocks through earth ground, the device was fully isolated. The ability of this device to detect nerve signals was thoroughly tested. Lastly, the ability of the device to isolate the test subject from earth ground was tested.

The second device designed measured the amount of time it takes for a finger to twitch after the nerve that innervates it is stimulated. The delay time between the stimulation and the finger twitching would then be used to assess the health of the nerve. This device was validated by testing it on a human. The ability of this device to detect nerve compression was thoroughly tested. The accuracy and consistency of this device were evaluated.

The final device designed was the stimulus device that was used by the two previous devices. This device produced a high voltage that caused nerves to generate action potentials. Like the other two devices, this device was validated by testing it on a human. The ability of this device to cause motor nerve action potentials was evaluated. This device was tested with different types of electrodes on several different locations on the hand and arm. It was tested on both the median and ulnar nerves. Testing conditions that caused minimal pain and burns were recorded.

1.5 Thesis Organization

The second section of this thesis provides background information about a wide range of different tests to assess nerve health. In addition, it provides more in-depth background information about nerve conduction studies. Lastly, it provides in-depth background information about stimulus devices used on nerves.

The third section of this thesis details the process of designing the three devices. The design process is described in chronological order. The first sixteen sections generally alternate between the development of the simple device to record action potential and the development of a stimulus device. The final four sections focus on the development of the device to measure motor responses. The results of all the experiments performed are given immediately after the experiments are described.

The fourth section contains a summary of all the results from the previous section.

The fifth section discusses the results and makes several recommendations for future research.

2. BACKGROUND

2.1 Methods of Assessing Nerve Health

There are many other medical devices to assess nerve health besides nerve conduction studies. Medical devices to assess nerve health devices are categorized based on the way they test a person's nerve health, the sensations they use, and the nerves they target [10].

The first way of categorizing nerve health assessing devices is by the way they function. Devices can be categorized as clinical, quantitative, or laboratory [10]. Clinical tests do not use precise inputs and rely on patient feedback [10]. For example, a doctor may press a cold object against a test subject's skin and ask them if they can feel it. This type of test generally uses the simplest equipment. Quantitative tests use precise inputs, but still rely on patient feedback [10]. For example, a doctor may apply a very specific amount of pressure against a test subject's skin and ask them if they can feel it. Laboratory tests do not require verbal feedback from the patient [10]. A nerve conduction study is an example of a laboratory test. This type of test generally uses the most complex equipment.

The second way of categorizing nerve health assessing devices is by the sensations they use to test a nerve. This categorization is primarily for clinical and quantitative testing devices. Sensitivity to touch, vibration, pinpricks, sharp pain, and temperature can all be used assess nerve health [10]. For example, tuning forks and Vibrameters use vibration to assess nerve health [10]–[12]. Temperature rollers use hot and cold stimuli to assess nerve health [10]. Neuropens use pinpricks to assess nerve health [10]. Semmes-Weinstein monofilament tests use precise levels of force against skin to assess nerve health [13]. Lastly, Neurometers use sinusoidal electrical signals to assess nerve health [14].

The third way of categorizing nerve health assessing devices is by the nerves they target. Some tests may specifically target sensory nerves or motor nerves. Motor nerves carry signals from the brain to muscles and glands. Sensory nerves carry signals from the somatosensory systems to the brain. Different types of sensory nerve fibers respond to different types of stimulus. Type Aβ sensory nerve fibers respond to sensations of touch and vibration [10], [11]. Type Aδ sensory nerve fibers respond to sensations of pinprick, sharp pain and cold [10]. Type C sensory nerve fibers respond to warmth and burning sensations [10]. Some electronic tests can select which nerve types they want to target by using different frequency stimuli [14].

2.2 Nerve Conduction Studies

The medical device of particular interest to this research is the nerve conduction device. When a nerve is stimulated by a nerve conduction device, it produces an electrical impulse known as an action potential. Action potentials can be measured as they are conducted along a nerve axon. The peak voltage and velocity of an action potential can be measured in order to detect neurological disorders. Nerves with damaged myelin sheaths generally have slower conduction velocities, and nerves with axonal degeneration generally have a lower peak voltage [2]. Unlike many other nerve health assessing tests, nerve conduction studies do not require feedback from the patient [10]. Not requiring patient feedback removes response bias from the results.

However, nerve conduction studies are susceptible to other causes of errors. The amplitude and velocity of an action potential can be affected by factors besides neurological health. The peak voltage and velocity of sensory nerve action potentials (SNAP) were found to vary from person to person based on gender and age [15]. These variances may be caused by differences in skin thickness and finger circumference [15]. Predictive models have been created to give more accurate action potential

amplitude and velocity reference values by incorporating relevant factors. Research found that predictive models incorporating certain physical characteristic such as age, gender, body mass index, and finger girth did not predict enough variance to be useful [16]. However, it suggested that results of nervous system tests could be made more accurate by running them multiple times and averaging the results [16].

Another factor that affects nerve conduction studies is temperature. The nerve conduction velocity has been estimated by older research to increase by 5 percent per degree Celsius of temperature increase from 29 to 38 degrees Celsius [17]. Newer research has shown that nerve conduction velocity does not increase linearly [1]. A standard temperature is often maintained in rooms where nerve conduction studies are performed in order to avoid variations in conduction velocity [17]. In non-standard temperature environments, the temperature should be recorded before testing and taken into account when the results are examined [17]. Temperature should be measured close to the area of stimulation [17]. The temperature should not be immediately changed before testing because this could introduce significant error into the results [17].

Lastly, nerve conduction studies can be performed both invasively and non-invasively. Non-invasive tests use surface electrodes while invasive tests uses near-nerve and on-nerve probes. Past research has shown that on-nerve invasive procedures produce larger action potentials [18]. However, the non-invasive procedures had faster nerve conduction velocities [18]. The on-nerve needle procedures were able to record sensory action potentials in more cases than the non-invasive procedures [18].

2.3 Optimal Stimulus Voltages

Both of the two testing devices developed over the course of this research required an electrical stimulus device. This stimulus needed to generate enough current through the body in order to cause nerves to generate action potentials. The minimum amount of current necessary to cause an action

potential is known as the threshold current. The amplitude of the generated action potentials should increase as the current increases above the threshold current [19]. Eventually, the amplitude of the generated action potentials stops increasing [19]. When the stimulus is greater than the amplitude necessary to generate a maximal nerve response, it is known as supramaximal [19].

The current necessary to have a supramaximal stimulus depends on the nerve and type of nerve fibers being tested. Previous research used 8 to 11 milliamps for median sensory nerves and 9 to 25 milliamps for median motor nerves [1]. The current generated by nerve conduction studies can be adjusted during testing in order to get an optimal nerve impulse. W. C. Wiederholt found that a 0.1 millisecond stimulus needed to generate a peak voltage of 80 to 110 volts in order to be supramaximal [19]. The average peak voltage of the stimuli created by commercial nerve conduction study devices was approximately 127 volts when the stimuli was set to generate 8 milliamps of current [20].

A second, undesirable action potential peak can appear if the stimulus current is not high enough [20], [21]. Moving the stimulating electrodes apart may also cause a second action potential peak [20]. Using a stimulus waveform with a long fall time can prevent a second peak from occurring [20]. Because of this, most commercially available nerve conduction studies use a stimulus waveform (Figure 1) that looks like a rounded rectangle and ends with an exponential decrease [20].

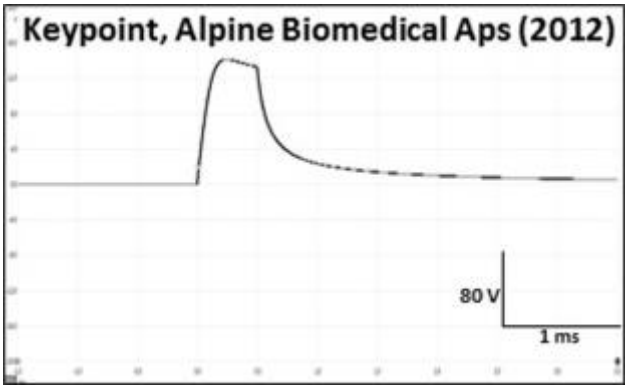

Figure 1: One of the stimulus waveforms recorded by Pereira et al. [20]

The energy required for a stimulus to activate a nerve is also affected by the shape of the stimulus waveform. Research has been done to assess the energy efficiency of several waveforms that may be used as stimuli [22], [23]. This research was initially performed using digital mammalian cell models [22]. Later, the stimuli were tested on live cats [23]. In the digital model tests, waveforms were assessed based their power efficiency, charge efficiency, and energy efficiency when stimulating nerves [22]. Power efficiency is a measure of instantaneous power required to reach a threshold. Charge efficiency is a measure of charge delivered to reach a threshold. Energy consumed is a measure of the total energy required to reach a threshold. The research did not find a single waveform to be the most power efficient, charge efficient, and energy efficient [22]. All three measures of efficiently were found to be strongly affected by the pulse width of the waveform [22].

The pulse width or duration of an electrical stimulus can affect both the efficiency of the stimulus and how much pain it causes. When determining the efficiency of stimuli with different durations, Wongsarnpigoon et al. tested different shapes of stimuli with durations from 0.01 to 5 milliseconds [22]. They did not find a stimulus duration that was most efficient for all the different waveform shapes they tested [22]. In a later study, they used waveforms from 0.02 to 2 milliseconds for testing on live cats [23]. When testing the relationship between stimulus duration and pain, Tamura et al. tested stimuli from 0.05 to 1 milliseconds [24]. They found that generally 0.2 milliseconds stimulus caused lower pain than other common stimulus widths [24]. When testing how the shape of a stimulus waveform affects its effectiveness, Pereira et al. used a stimulus duration of 0.5 milliseconds for all his tests [20]. However, their stimulus ended with a long voltage decay that roughly lasted for an additional 0.8 milliseconds [20].

3. METHODS

3.1 Arbitrary Waveform Generation

This research began by developing ideas for the stimulus device. The plan was to use an arbitrary waveform generator with a waveform created in a computer program as a stimulus. A waveform was designed in Matlab (Figure 2) based on six waveforms used by commercially available nerve conduction study (NCS) devices [20]. The characteristics incorporated into this waveform were: a sharp start to the rising edge, a rounded end to the rising edge, a downward sloping plateau, a sharp start to the falling edge and a rounded stop to the falling edge [20]. It was expected that the amplitude would need to be approximately 120 volts and the duration would need to be 1.0 to 1.5 milliseconds for this waveform to stimulate the median nerve.

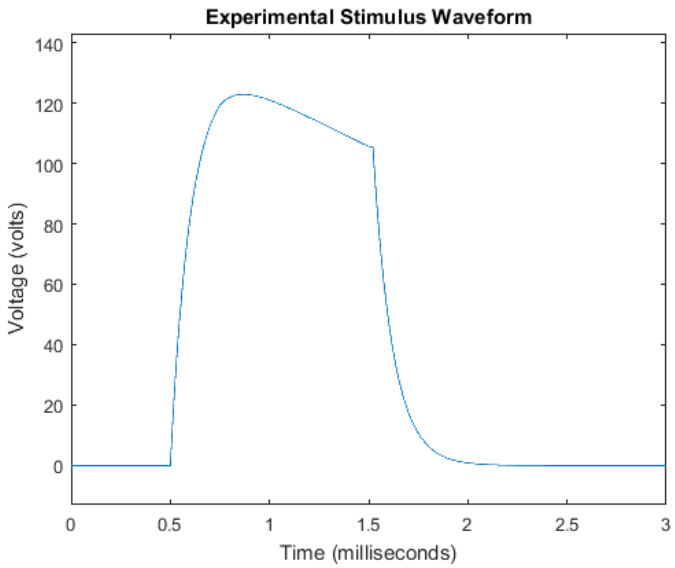

Figure 2: Stimulus waveform shape that was created based on the six stimulus waveforms measured by Pedro Pereira et al [20]. It was created using the program Matlab

From Matlab, the waveform was exported as raw numerical data values in a comma-separated values (CSV) file. Next, the waveform data values were imported to BK Precisions WaveXpress software (Figure 3) where they were saved as a B&K Precision waveform (BKW) file.

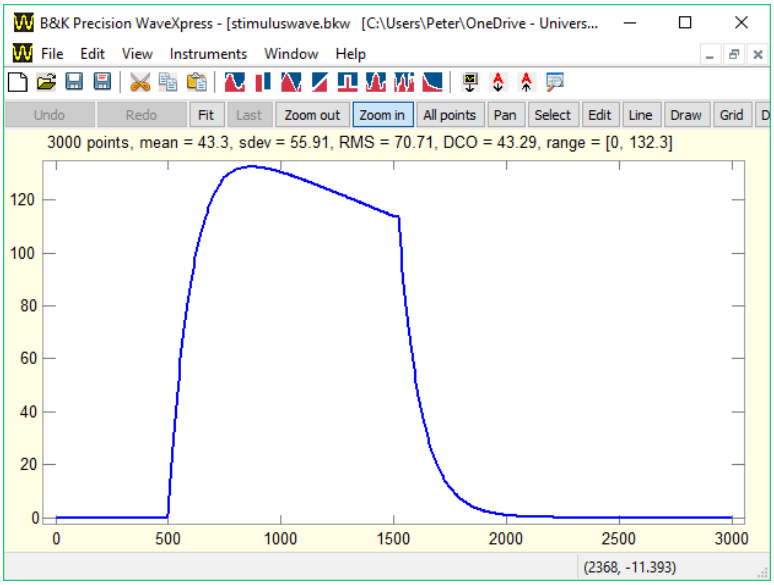

Figure 3: Stimulus waveform created by importing data into the BK Precision WaveXpress software

A BK Precisions 4054 arbitrary waveform generator was going to be used to generate the waveform. However, after consulting the specifications sheet for the BK Precision 4054, it was determined that its peak output was only 5 volts [25]. This was significantly less than the 120 volts peak that the stimulus required. An Agilent (Now Keysight) 33500B series arbitrary waveform generator was also available to use. However, it was determined that the Agilent waveform generator only had a peak output of 10 volts [26]. Since a high voltage arbitrary waveform generator was not available, the idea of rapidly repeating the stimulus many times at a lower voltage to stimulate the nerve was considered.

3.2 High Frequency Waveform Testing

Testing was done with basic pulse waves of different amplitudes, duty cycles and frequencies to determine if a low-voltage stimulus could generate enough current to stimulate the nerve. Since previous research required as much as 25 milliamps of current to cause an action potential in the median motor nerves [1], the goal was to generate that much current with this stimulus. Since the Agilent waveform generator only had a peak voltage of 10 volts, generating this much current would require reducing the skins impedance to 400 ohms. A square wave was used because previous research found it was the most power efficient across a range of different pulse widths [22]. Testing was performed on the wrist using foam-gel silver/silver chloride electrodes.

Current and impedance measurements were taken as the frequency of the stimulus square wave was incremented by a magnitude of ten from 1 hertz to 100,000 hertz (Table 1 and Figure 4). The peak voltage was kept constant at 1 volt, and the duty cycle was kept constant at 50%. Testing was only performed once for each frequency meaning the current and impedance values may not be very precise. However, it could be clearly seen that increasing the frequency caused the skin impedance to decrease and the current through the body to increase. This matches the general conclusion reached by a past scientific research test [27]. The lowest impedance was recorded when stimulating at 100,000 hertz. However, even at 100,000 hertz, the impedance was still almost double the limit of 400 ohms.

Frequency	Voltage	Current (milliamps)	Impedance
100000	1	1.3144	760.8
10000	1	0.8060	1240.7
1000	1	0.2785	3590.7
100	1	0.1024	9765.6
10	1	0.0611	16366.6
1	1	0.0486	20576.1

Table 1: Measured current and impedance from 100 kilohertz to 1 hertz

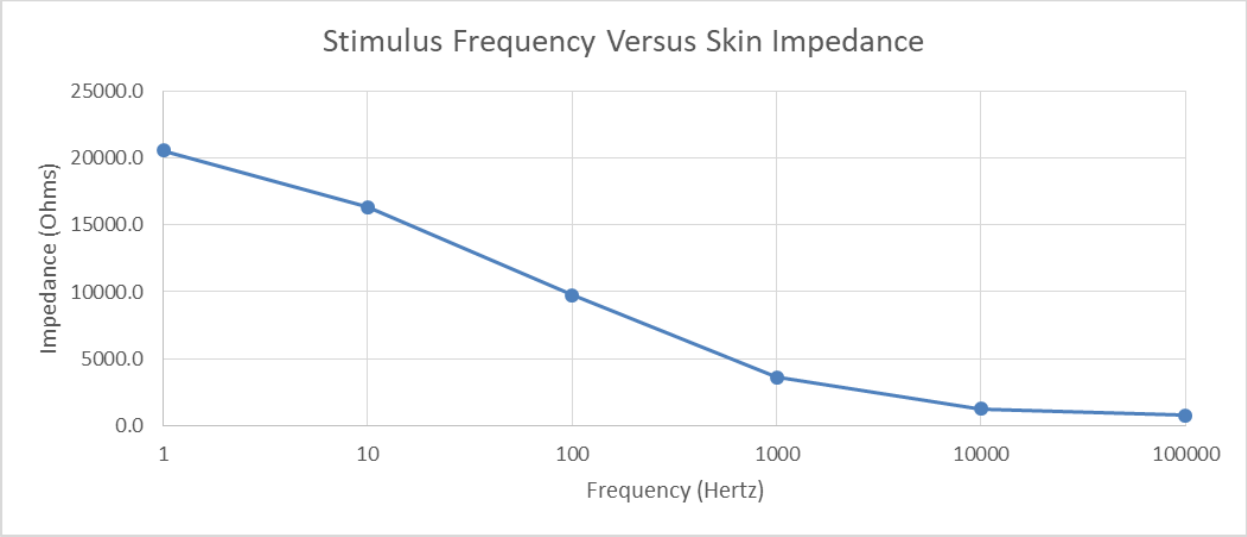

Figure 4: Stimulus frequency versus skin impedance from 1 hertz to 100 kilohertz

Some additional testing was performed with the 100,000-hertz stimulus to confirm it could not generate median motor nerve action potentials. The presence of median motor nerve action potentials was confirmed by observing the thumb for muscle activations. After the stimulus failed to generate any motor action potentials, the idea of using such a high frequency, low-voltage stimulus was abandoned. The plan to use an arbitrary waveform generator to generate the stimulus was also abandoned. Instead, the focus of the research shifted towards designing custom circuit that could generate a high voltage stimulus.

3.3 Designing a Suitable Bio-Amplifier

In order to observe nerve action potentials, a high gain, low noise bio-amplifier was required. A custom bio-amplifier was built based on a bio-amplifier design used in the Biomedical Instrumentation class at University of New Hampshire [28]. This bio-amplifier consisted of five stages: an instrumentation amplifier, a high-pass filter, a gain stage, an isolation amplifier, and a low-pass filter (Figure 5).

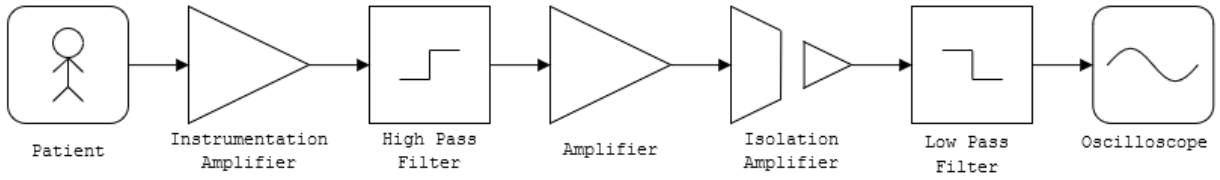

Figure 5: Block diagram of the bio-amplifier design

The low-pass and high-pass filter cutoff values were selected based on values used by nerve conduction devices in other scientific papers. Values were collected from eleven other scientific papers (Table 2). Since 20 Hz was a common cutoff for the high-pass filters, it was used for this bio-amplifier. Likewise, 2000 Hz was selected as the low-pass cutoff frequency.

High-Pass Filter Cutoff	Low-Pass Filter Cutoff	Source
0.1 hertz	2 kilohertz	[19]
1 hertz	3 kilohertz	[22]
1 hertz	3 kilohertz	[23]
1.6 hertz	2 kilohertz	[17]
5 hertz	5 kilohertz	[29]
5 hertz	10 kilohertz	[21]
10 hertz	3 kilohertz	[24]
20 hertz	2 kilohertz	[18]
20 hertz	2 kilohertz	[13]
20 hertz	2 kilohertz	[16]
20 hertz	2 kilohertz	[20]

Table 2: Low-pass and high-pass filer cutoff values used in other research papers

The bio-amplifier was designed to amplify both motor and sensory nerve signals. However, because there was such a large amplitude difference between motor and sensory nerve signals, the gain of the bio-amplifier would have to be different for each signal. Past research found that median motor nerve signals are generally a few millivolts in amplitudes while median sensory nerve signals generally are tens of microvolts in amplitude [30]. The bio-amplifier gain was initially set so that the bio-amplifier would output 1 volt when the input was 33 microvolts. This would make the bio-amplifier suited for detecting

sensory nerve signals. If necessary, the gain could be adjusted later to make it more suitable for detecting motor nerve signals. To reach this level of amplification, the entire bio-amplifier required a gain of 30,000. This gain was split between the first and third stages of the bio-amplifier.

The first stage of the bio-amplifier was an instrumentation amplifier. An INA 128 precision, low-power instrumentation amplifier was used. This amplifier was designed for use in medical instrumentation [31]. Instrumentation amplifiers have high bandwidth even when their gain is high [31]. The gain of this amplifier was set to 200.

The second stage of the bio-amplifier was a high-pass filter. A fourth-order Sallen-Key high-pass filter was used. This was made from two second-order high-pass filters with the Q factors of 0.541 and 1.306 respectively. These Q factors were selected because they gave the filter a Butterworth response, which has a pass-band with maximum flatness. The equations for this filter were derived from a circuit diagram and the values of every resistor and capacitor were calculated using those Q factors. A Matlab program was written to verify the calculated values (Appendix: Program 1). The amplifier IC used to implement this stage was an LM 324 Quad Operational Amplifier. This amplifier was selected because it was readily available.

The third stage of the bio-amplifier was a gain stage. Given that the previous stage had gain of 200 and the overall gain need to be 30,000, this stage was given a gain of 150. The amplifier IC used to implement this stage was also an LM 324 Quad Operational Amplifier.

The fourth stage of the bio-amplifier was the isolation stage. This stage separated the previous three bio-amplifier stages electrically from the remaining stages using an ISO124P isolation amplifier. The input side of the isolation amplifier and the previous three stage were all powered by two 9-volt batteries. This meant the test subject's body was never directly connected to earth ground. This stage was crucial because it prevented the stimulus circuit from grounding to the bio-amplifier. Because the

two side of the isolation amplifier were separate, powering the output side of the isolation amplifier and all subsequent stages with a 12-volt bench supply did not connect the test subject to earth ground.

The fifth stage of the bio-amplifier was a low-pass filter. A second-order Sallen-Key low-pass filter was used. It had a Q factor of 0.737, which gave it a Butterworth response. Just like with the high-pass filter, the equations for this filter were derived from a circuit diagram and verified using Matlab (Appendix: Program 2). The amplifier IC used to implement this stage was also an LM 324 Quad Operational Amplifier.

3.4 Processing Data from the Bio-Amplifier

The output of the bio-amplifier was connected to an Agilent Technologies InfiniiVision DSO-X 3014A oscilloscope. From there, it was exported as a CSV file. The maximum number of samples points that the oscilloscope could save in a single file was 62,500 per waveform. In cases where the waveform duration is shorter than 0.0625 seconds, the output file has a maximum sample rate of 1,000,000 samples per second. However, in cases where the waveform duration is longer than 0.0625 seconds, there was down sampling to keep the file smaller than 62,500 samples.

The data in the CSV files was analyzed and graphed in Matlab. The first two rows of the CSV file contained unnecessary technical information and were discarded. The first column of the CSV file contained timescale data. The remaining one to four columns contained voltage recordings from a channel of the oscilloscope.

A program was written to graph the waveforms (Appendix: Program 3). The graphs were automatically labeled and saved as portable network graphics (PNG) files. If the CSV file contained multiple

waveforms, it would plot them on separate graphs in the same image. All the images of the waveform were saved along with the CSV file and a description of the test performed.

3.5 Removing 60-hertz Noise

After these five stages were completed, some simple testing of the bio-amplifier was performed. The first tests of the bio-amplifier were performed using the Agilent waveform generator to create a stimulus. A 20-hertz pulse wave with a 10-volt peak and 10% duty cycle was used as a stimulus. Silver/silver chloride foam-gel electrodes were used for both the stimulating electrodes and the recording electrodes. The skin was cleaned with 73% isopropyl alcohol before applying electrodes.

Stimulating electrodes were placed on the middle finger so that they would target the median sensory nerve (Figure 6). Pereira et al. also placed the stimulus electrode on the middle finger and the recording electrodes on the wrist [20]. The positive electrode was placed on the middle phalanx and the negative electrode was placed on the proximal phalanx. The recording electrodes were placed on the ventral side of the arm above the median nerve. The positive recording electrode was placed one inch below the crease of the wrist and the negative recording electrode was placed two and a half inches below the crease of the wrist. The ground recording electrode was placed in the middle of the back of the hand.

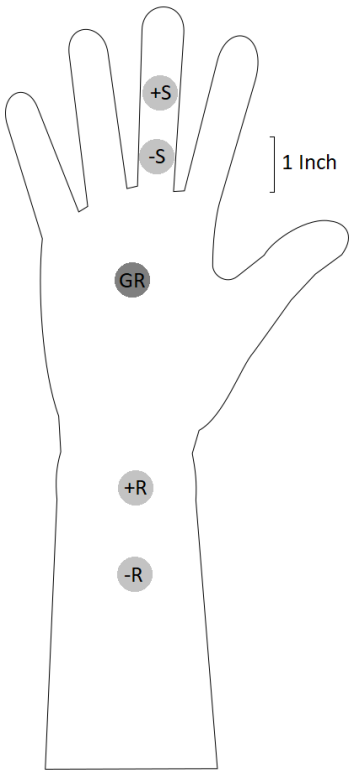

Figure 6: Placement of electrodes on the hand. The "–R" symbol represents the negative recording electrode. The "+R" symbol represents the positive recording electrode. The "GR" symbol represents the ground recording electrode. This electrode is dark grey because it was place on the back of the hand. The "–S" symbol represents the negative stimulating electrode. The "+S" symbol represents the positive stimulating electrode

The bio-amplifier produced an output when using the waveform generator as a stimulus. The first recordings from the body appeared to be mostly 60-hertz noise with some random noise and periodic bumps (Figure 7). The periodic bumps appeared to be an artifact of the stimulus because they occurred at the same time as the stimulus. In order to measure the amount 60- hertz noise, a program that performs a Fourier spectral analysis and a power spectral analysis was written (Appendix: Program 4). The analysis revealed that most of the signal was 60-hertz noise (Figures 9 and 11).

After the initial testing revealed the recordings contained significant 60-hertz noise, a filtering program was written (Appendix: Program 5). This program was designed to filter out the low frequency components of the waveform. It used a 20-hertz fourth order Butterworth high-pass filter to remove the

noise. After being filtered, one of the initial tests had clearly visible peaks where the stimulus occurred (Figure 8). A Fourier spectral analysis and a power spectral analysis were performed on the filtered waveform to show the 60-hertz noise reduction (Figures 10 and 12).

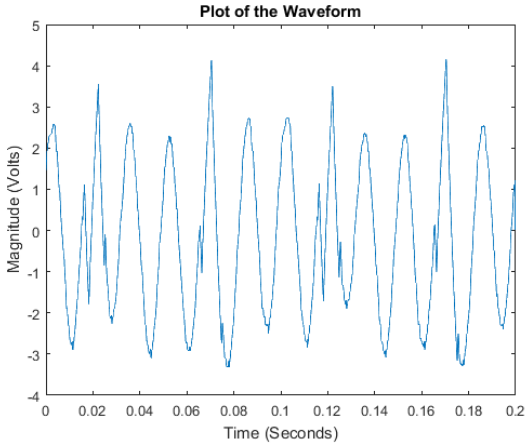

Figure 7: One of the initial recordings from the body

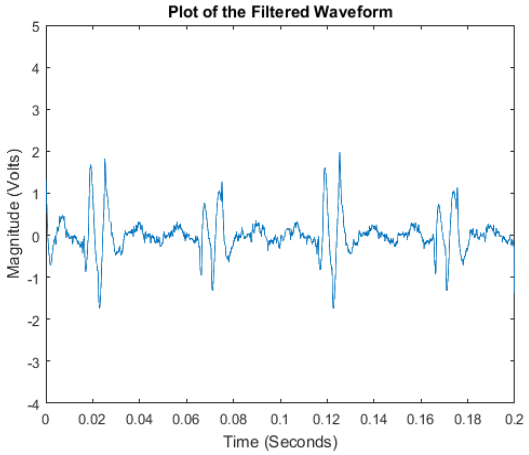

Figure 8: The same recording after being filtered

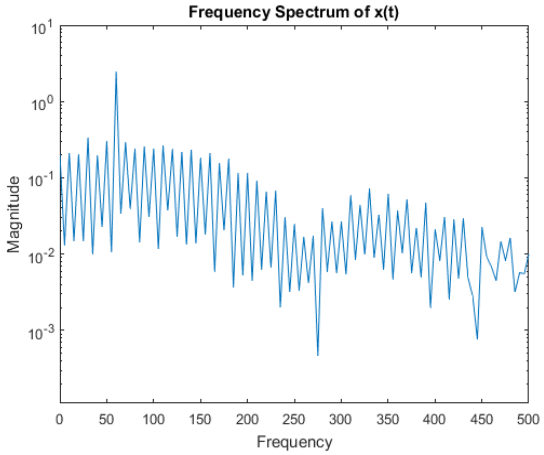

Figure 9: Frequency spectrum analysis of the initial recording. There is a voltage spike at 60-hertz

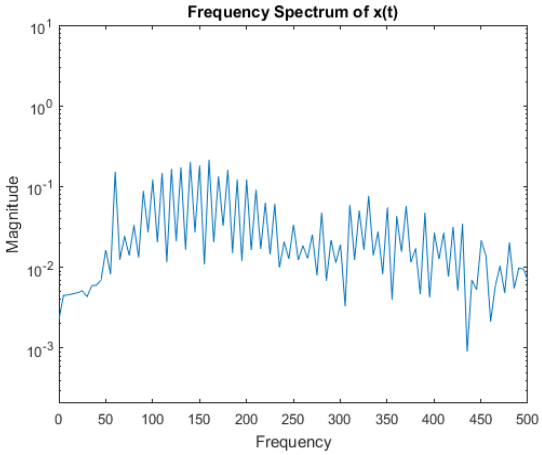

Figure 10: Frequency spectrum analysis of the filtered recording. The voltage spike at 60-hertz has been reduced

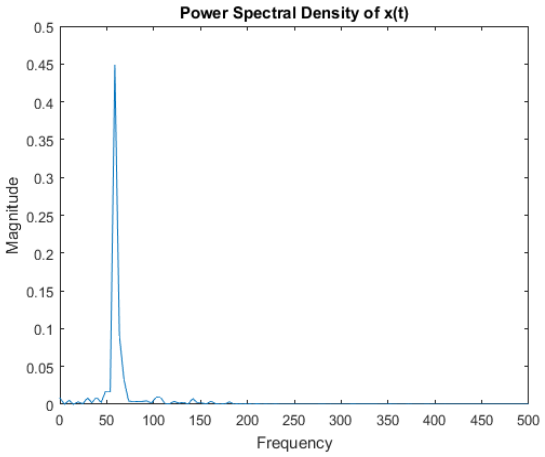

Figure 11: Power spectrum analysis of the initial recording. There is a power spike at 60-hertz

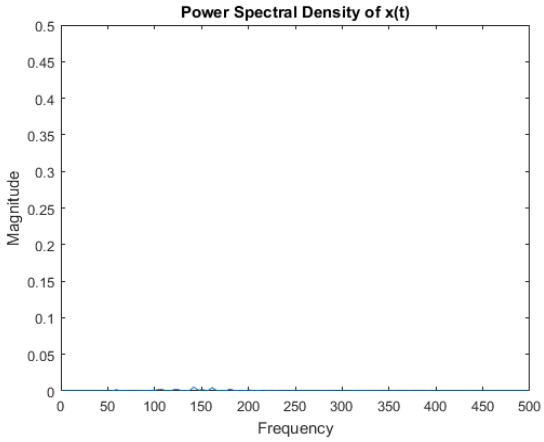

Figure 12: Power spectrum analysis of the filtered recording. The power spike at 60-hertz is no longer present

To address the significant 60-hertz noise, a sixth stage was added to bio-amplifier. The sixth stage was a twin-t 60-hertz notch filter. A new block diagram was created with the notch filter added (Figure 13).

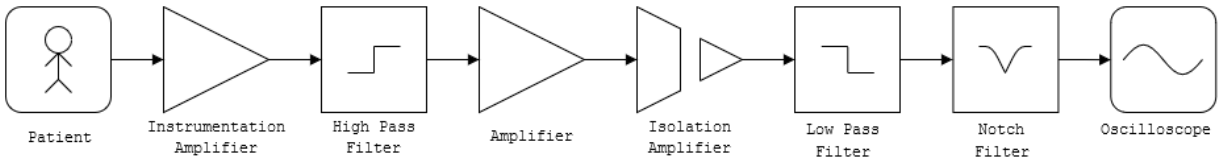

Figure 13: Updated block diagram of the bio-amplifier design

A circuit diagram of the completed circuit was drawn using the website Draw.IO (Figure 14). A Multisim 13 design of the circuit was also created (Figure 15). In the version of Multisim used, LM 324 and ISO 124 were not available. The 741 amplifiers were used in place of the LM 324 amplifiers, and an ISO 130 was used in place of ISO 124. The frequency response of this circuit was graphed using Multisim (Figure 16).

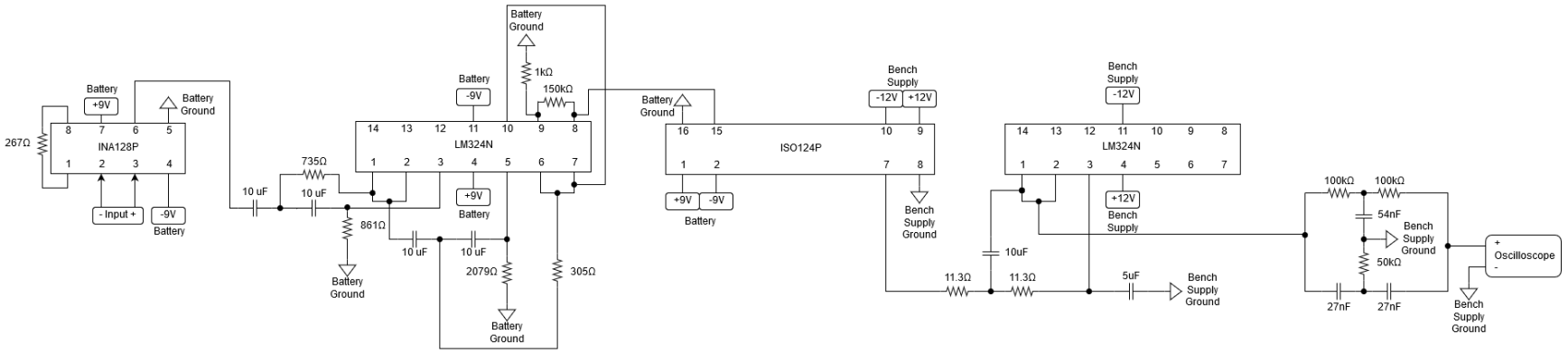

Figure 14: Circuit diagram of the updated bio-amplifier

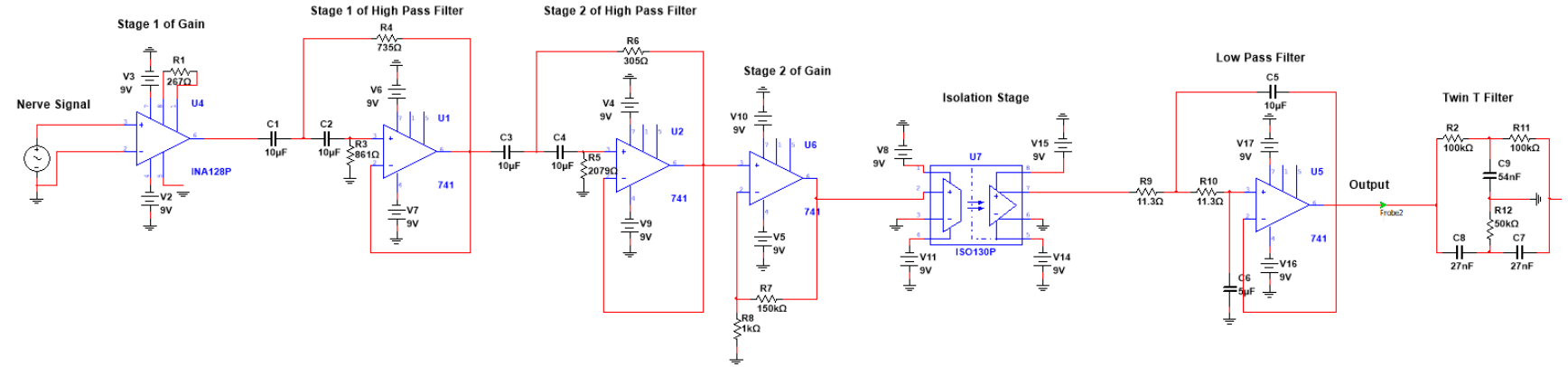

Figure 15: Multisim 13 design of the updated bio-amplifier

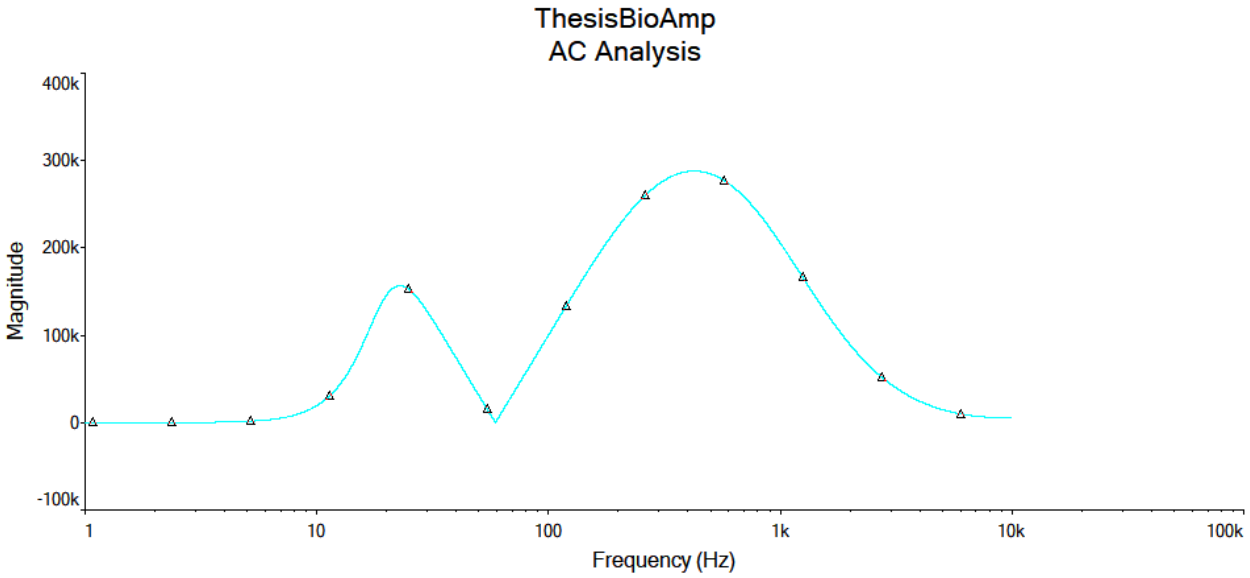

Figure 16: Simulation of the frequency response of the updated bio-amplifier

3.6 Removing Random Noise

There appeared to be a nerve response visible in the body when the stimulus was applied. However, this response was not clear because of random noise. Because the recordings contained significant random noise, a second graphing program was written (Appendix: Program 6). This program was designed to reduce random noise by averaging multiple responses together. It could average responses from the same waveform recording as well as responses from different waveform recordings. It accepted input files with single waveforms containing five responses. Five responses were generated by stimulating the arm using a 1-hertz stimulus over five seconds. The graphing program also reduces 60-hertz noise by filtering the waveforms with a Butterworth band-stop filter. The low frequency cutoff of the band-stop filter was 59 hertz and the high frequency cutoff was 62 hertz.

The averaging program had three different ways of averaging the waveforms in order to make the responses clearer (Figures 17 through 20). The first way was to break the waveform into five equally

sized parts and then average them together (Figure 17). This method works because the stimuli occurred periodically with exactly the same delay between each stimulus. In theory, when the waveform is divided into five pieces, there should be a response in each piece and the response should start at the same time in each piece. In practice, there was a slight difference between when each response started.

The second way of averaging was to break the waveform into fifths and align each part by the highest (or lowest) point before averaging (Figures 18 and 19). The response that appeared immediately after stimulating appeared to be shaped like a peak immediately followed by a valley. The highest (and lowest) point of the waveform occurs during the response. Aligning waveforms by their highest (or lowest) point essentially aligned them by the responses and made the responses clearer. However, because the waveforms were aligned based on their highest (or lowest) point, their amplitude at this point was exaggerated. This distorted the shape of the response by creating sharp peaks.

Once the distortion was discovered, a third way of averaging was used instead (Figure 20). The third way of averaging aligned the responses by the zero crossing that occurs between the high and low points of the response. Because the responses were aligned at a zero point, this method of alignment did not result in exaggerated peaks.

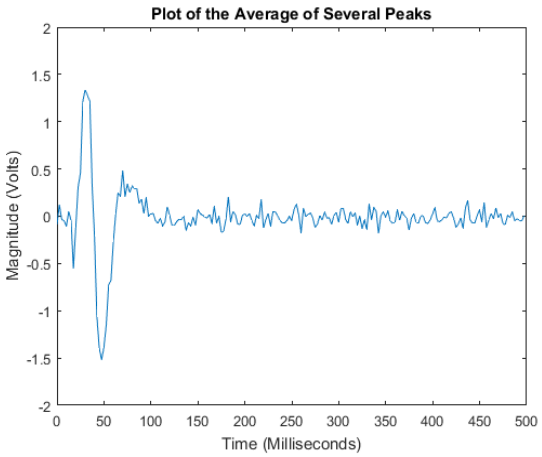

Figure 17: The averaged waveform that was not aligned

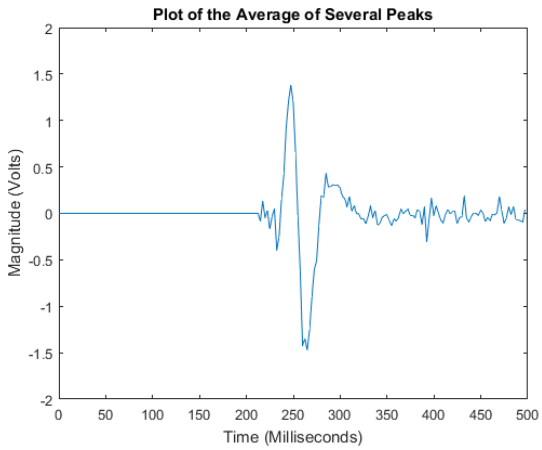

Figure 18: The averaged waveform aligned by the highest point. The peak of this waveform is slightly higher

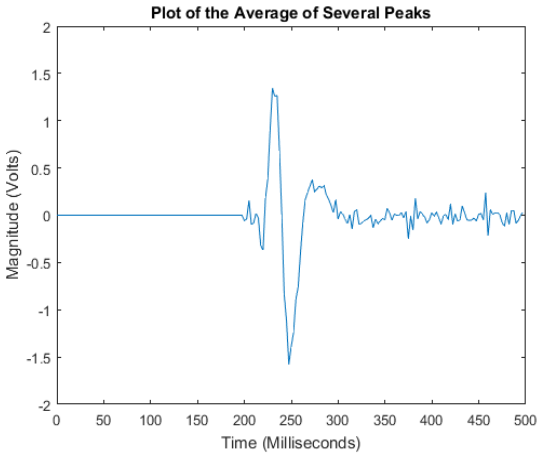

Figure 19: The averaged waveform aligned by the lowest point. The valley of this waveform is slightly lower

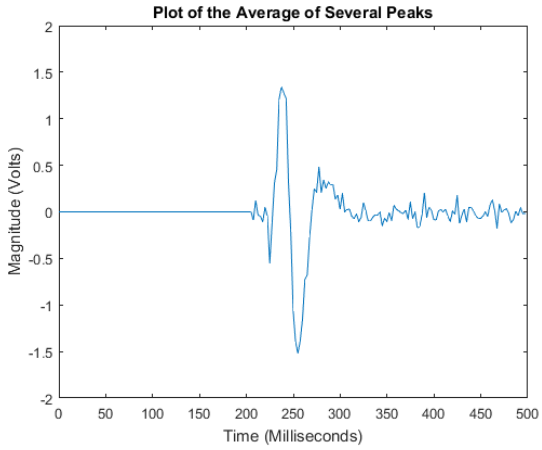

Figure 20: The averaged waveform aligned by the center point. The peaks of this waveform are the same as the non-aligned waveform

The number of samples that each of the five responses (Figures 17 through 20) was shifted before being averaged was recorded (Table 3). In the unaligned average and the middle aligned average did not shift any of the responses before averaging. The highest point aligned average shifted the last three responses right by one value each. The lowest point aligned average shifted the first three responses right by one value each.

Response #	Unaligned Average	Highest Point Aligned Average	Lowest Point Aligned Average	Middle Aligned Average
Response 1	0	0	1	0
Response 2	0	0	1	0
Response 3	0	1	1	0
Response 4	0	1	0	0
Response 5	0	1	0	0

Table 3: The number of samples that each response was shifted in order to align under each alignment system

Since multiple responses were being recorded in a single waveform, another program was written to select and graph the individual responses separately. The program plots the entire waveform using sample number for the x-axis instead of time (Figure 21). This allows the user to view waveform and determine at what sample responses occur. The user enters the center of the first response, width of the first response, and the number of responses in the waveform. Using this information, the program displays all the responses on their own graphs (Figure 22). It displays the other responses by assuming each response is equally spaced. If a periodic stimulus is used, this will occur.

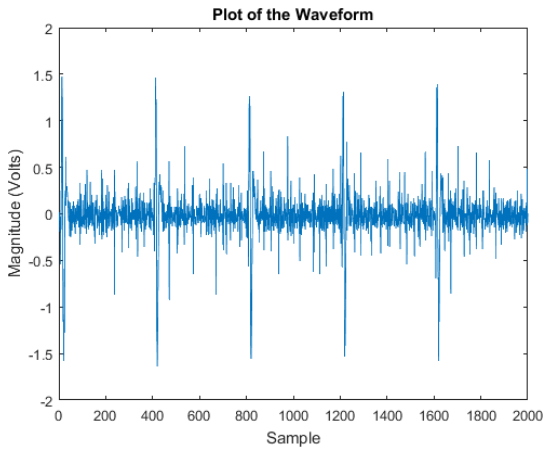

Figure 21: Graph of a whole waveform using the sample number as x-axis

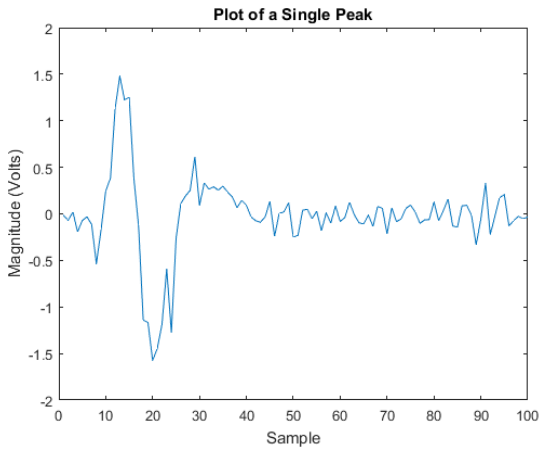

Figure 22: Graph of a single response from the waveform using the sample number as x-axis

3.7 Fixing Test Subject Isolation

A problem was encountered with the bio-amplifier during testing with a 1-hertz stimulus. The stimulus could be felt jumping from the stimulus electrodes to the bio-amplifier electrodes. To confirm this was happening, the negative stimulus lead was removed from the test subject's skin. This should stop the stimulus pulse from entering the test subject's body if their body was properly isolated. However, the stimulus pulse could still be felt entering the body after the lead was removed.

Testing showed that the isolation had been broken in several places (Figure 23). The first place that the isolation was broken was at the test subject's arm. The test subject's arm had been placed on a conductive mat to reduce outside noise. However, this conductive mat was connected to earth ground. Removing the conductive mat and placing the test subject's arm directly on the testing bench was considered. However, it was found that the surface of the testing bench still had a connection to earth ground. In order to prevent the test subject's arm breaking isolation, all further tests were done with the test subject holding their arm in the air.

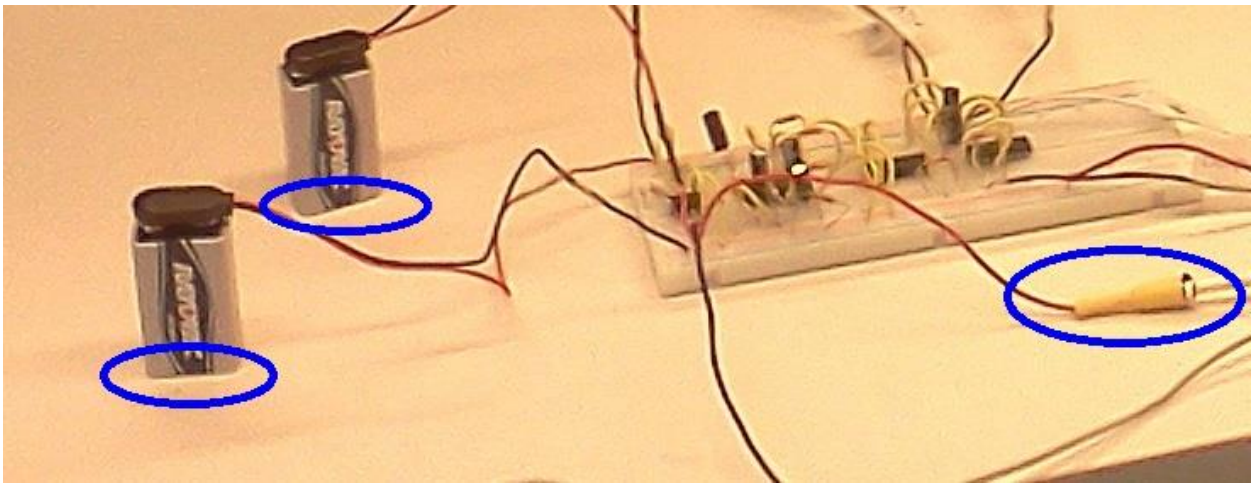

Figure 23: The areas circled in blue are places were isolation was broken. The two batteries on the left broke isolation by touching the table. The wire adapter on the right also broke isolation by touching the table

The second place that isolation had been broken was where the batteries of the bio-amplifier touch the table. This was fixed by placing the batteries and the bio-amplifier circuit on an insulated board.

The third place that isolation had been broken was the hardest to find. After some extensive testing, it was determined that the isolation was broken where a wire adapter touched the surface of a table. The snap leads connected to the electrodes on the body had a 2-millimeter pin on their opposite end. A 2-millimeter pin to 28-gauge wire adapter was needed between each of the bio-amplifier leads and the bio-amplifier circuit. One part of the adapters was not insulated and was touching the surface of the table causing the bio-amplifier be connected to earth ground. To fix this, these adapters were replaced with properly insolated adapters.

3.8 Electromagnetic Noise

The response recorded from wrist (Figure 24) appeared to be the same shape as a nerve action observed in previous research (Figure 25) by Aprile et al. [21]. It appeared to be a median nerve response.

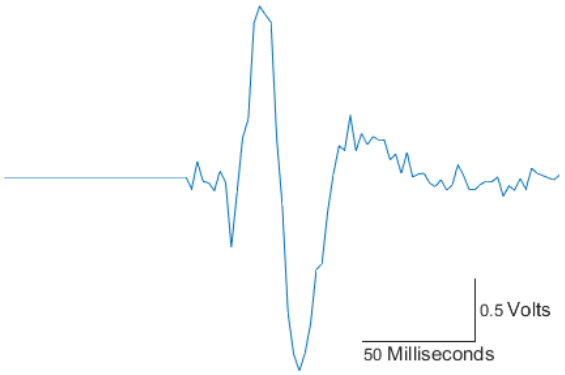

Figure 24: The average response recorded from the wrist after stimulating

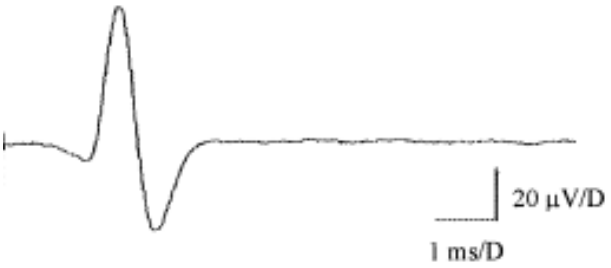

Figure 25: Sensory nerve action potential recorded by Aprile et al. [21]

However, the response lasted much longer than it should have. It lasted around fifty milliseconds while a sensory nerve potential should only last around two milliseconds.

When the stimulus electrodes were moved from the median nerve in the center of the wrist to the side of the wrist, the response continued to show up. If it was a nerve response, it should have disappeared because the nerve was no longer being stimulated.

It was suspected that stimulus was traveling across the surface of the skin. The bio-amplifier had an isolation stage to prevent this from happening. The isolation stage of the bio-amplifier was checked by removing the negative lead of the stimulus. When the negative lead was removed, the stimulus stopped. If the isolation was not working, the stimulus would have been grounded by the bio-amplifier and continue to flow through the body.

When device was tested without any stimulus leads connected, a response could still be seen in the output. It was thought that this interference was electromagnetic interference caused by electromagnetically coupling of the stimulus leads and the bio-amplifier leads. To test this, the stimulus circuit was placed on the opposite side of the testing bench from the bio-amplifier. This meant the two circuits and their wires were about three feet apart. The response disappeared completely, which confirmed that the output was from electromagnetic interference.

3.9 Non-electrical Stimulus

Since the electrical stimuli caused electromagnetic noise, non-electrical stimuli were considered. Testing was done to determine if a non-electrical stimulus could generate detectable nerve impulses. To generate the sensory nerve impulses, the middle finger was prodded repeatedly with a 28-gauge wire. However, there was no significant difference between the output from this test and the control test.

3.10 High Voltage Stimulus

Subsequent work was resumed on a higher voltage stimulus. The first approach tested used a transistor connected to two DC power supplies (Figure 26). The combined voltage of the two DC power supplies was 55.6 volts. Using the Agilent waveform generator, a pulse waveform that was high for only a short duration could be generated. However, this stimulus generated significant heat in the 1k resistor and was unsafe for human testing. Furthermore, this stimulus voltage did not meet the 90-volt stimulus goal.

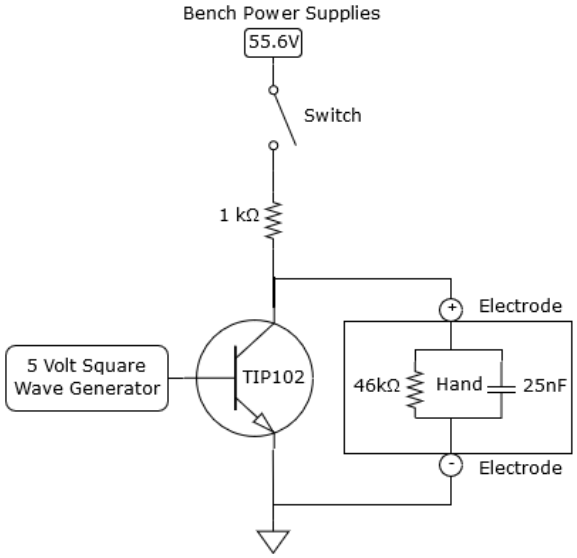

Figure 26: Circuit diagram of the prototype stimulus. The resistance and capacitance of the hand is represented by the 46 kiloohm resistor and the 25 nanofarad capacitor

Because of these problems, a new stimulus circuit which used an inductor to generate a high voltage stimulus was tested (Figure 27). One end of the inductor was connected to a bench power supply. The other end was connected to three elements in parallel with the ground: a transistor, the test subject's hand, and a voltage divider.

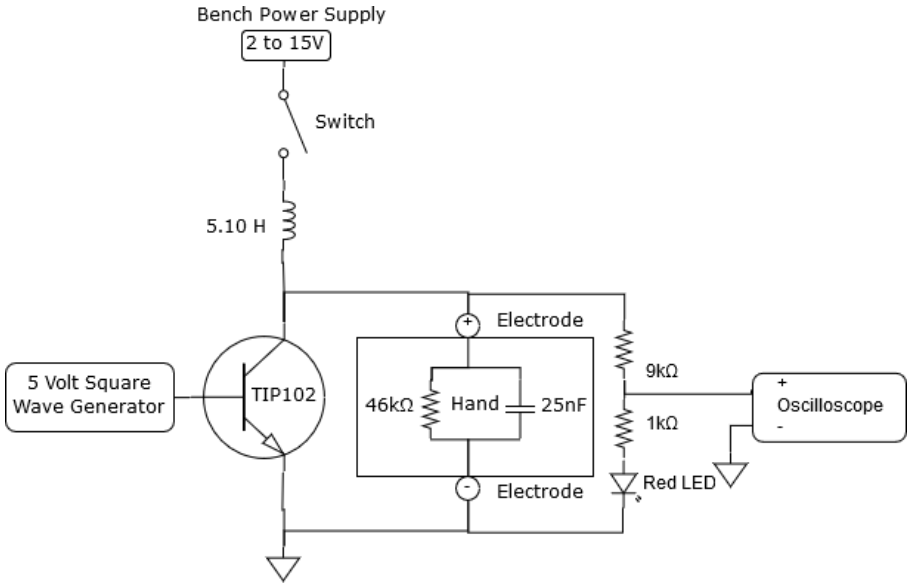

Figure 27: Circuit diagram of the inductor-based stimulus. The resistance and capacitance of the hand is represented by the 46 kiloohm resistor and the 25 nanofarad capacitor

The transistor connected the inductor to ground and it was controlled by a pulse generator. The pulse generator produced a 1-hertz, 0-to-5 volt square wave with an 8.4 nanosecond rise time. The periodic switching of the transistor from open to closed resulted in a high voltage peak being generated by the inductor (Figure 28). When the transistor was closed, the circuit produced a DC voltage, which came from the bench power supply.

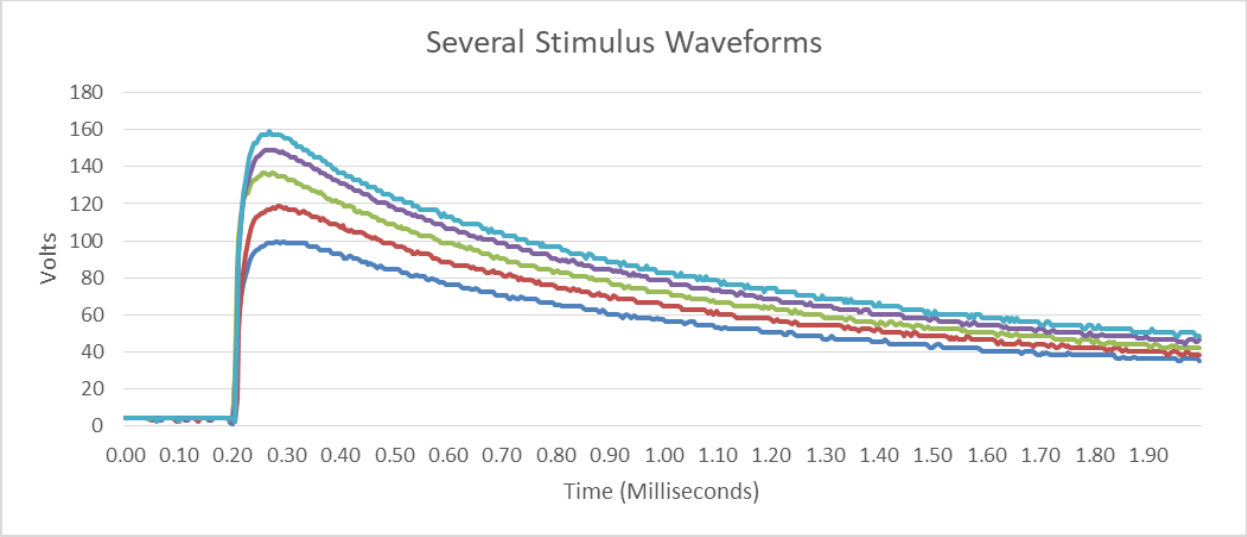

Figure 28: Overlay of several high voltage peaks created by the inductor-based stimulus. The difference in peak voltage is caused by changing the DC power supply voltage

Several inductors with inductances varying from 0.1 millihenries to 5.1 henries were tested to see which generated the best stimulus. Each inductor was given enough input voltage to generate a 120-volt stimulus. The primary difference between the inductors was how long they could maintain that voltage. Approximations of the stimulus durations of each inductor were recorded (Table 4). The duration was measured halfway between the start of the peak to the top of the peak. Because all the waveforms were roughly the same shape these values could be compared to each other. However, if the waveforms were different shapes, a more precise method of comparison would have been necessary. The theoretical stimulus duration for each inductor was calculated for comparison (Table 4).

Inductor	Stimulus Duration	Theoretical Stimulus Duration
0.1 mH	0.5 µS	0.0122 µS
1 mH	1 µS	0.1217 µS
33mH	5 µS	4.017 µS
100 mH	10 µS	12.17 µS
1 H	75 µS	121.7 µS
5.1 H	474 µS	620.9 µS

Table 4: Rough approximation of the duration of the stimulus peak by inductor used as well as the theoretical stimulus duration

The theoretical stimulus duration was estimated for each inductor using the time constant for a series RL circuit (Equation 1). The time constant represents the amount of time it takes for the voltage across the inductor to fall to 1/e or 36.8% of its starting voltage. In this case, the resistance "R" in the time constant equation represents the equivalent resistance of the two resistors in the voltage divider and the resistance of test subject's hand. Using the time constant, the voltage across the inductor as it discharges can estimated (Equation 2).

$$\tau = \frac{L}{R}$$

Equation 1: The time constant for a series RL circuit

$$V_L(t) = Ve^{-\frac{t}{\tau}}$$

Equation 2: The instantaneous voltage across a discharging inductor in a series RL circuit

In half of the cases, the measured stimulus duration values are larger than the theoretical values, while in the other half they are smaller. The stimulus duration measurements were taken at 50% of the peak stimulus voltage, which may be why they do not match the theoretical values exactly. In addition, the capacitance of the hand was not incorporated into the calculation of the theoretical values.

At this point, the previous goal to have a 1.0 to 1.5 millisecond stimulus was reconsidered. Pereira et al. used stimulus that was only 0.5 milliseconds long [20]. Tamura et al. tested stimuli from 0.05 to 1 milliseconds [24] and Wongsarnpigoon et al. tested stimuli from 0.02 to 2 milliseconds [23]. Based on this research, a shorter stimulus duration was considered. A stimulus duration of 0.1 to 1.5 milliseconds was selected as the new, more flexible goal. The 5.1-henry inductor was selected because it generated a

peak that lasted almost 0.5 milliseconds. The 5.10 henry inductor was the primary side of a Tamura 3FS-310 Laminated Power Transformer.

The peak voltage and stimulus duration of the 5.10 henry inductor could be controlled by adjusting the voltage of the bench supply. Voltages from 41.8 volts to 135 volts were generated by adjusting the bench supply voltage from 2 volts to 15 volts (Figure 29). The duration of the stimulus varied from around 0.5 milliseconds to 1 millisecond as the supply voltage was increased. When the bench supply voltage was below 2 volts, the inductor did not generate a high volt spike. When the output was roughly 135 volts or higher (the input voltage was 15 volts or higher), the inductor generated voltages that were painful for the test subject. When the output was about 95 volts or higher (the input voltage was 7 volts or higher), the inductor would cause a finger to twitch. Individual fingers could be targeted by moving the position of the stimulation electrodes on the wrist.

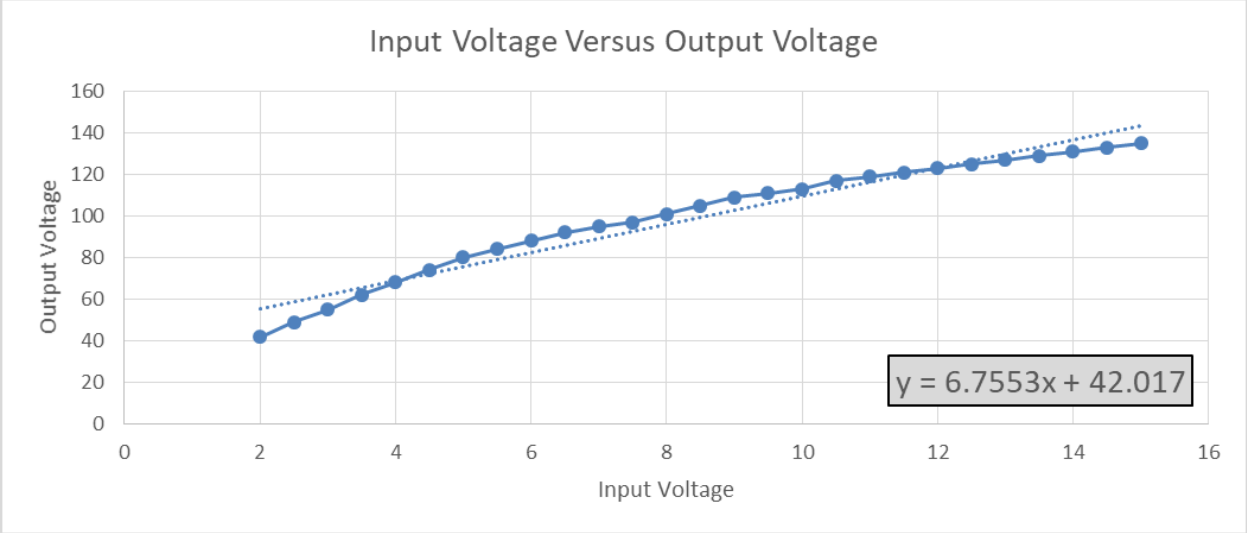

Figure 29: Graph of the input voltage versus the output voltage

Besides being connected to the test subject, the stimulus voltage was also connected to a voltage divider. The voltage divider reduced the stimulus by a factor of 10 (Equation 3). The output of the voltage divider was connected to an oscilloscope. It was necessary to reduce the voltage because the

oscilloscope could only display up to 20 volts. With the reduction, the voltage output to the oscilloscope was between 4 to 13.5 volts.

$$V_{out} = \frac{1\ k\Omega}{1\ k\Omega + 9\ k\Omega} V_{in} = \frac{1}{10} V_{in}$$

Equation 3: The equation for the output voltage of the voltage divider

Later, a standard red light-emitting diode was placed between the voltage divider and ground. This light-emitting diode blinked when the stimulus circuit was active. This was done as a safety precaution. It was assumed that the forward voltage of the light-emitting diode was the standard 1.8 volts. The equivalent resistance of the light-emitting diode changes depending on the input voltage (Equation 4). The light-emitting diode changes the output voltage of the voltage divider depending on the input voltage (Equation 5).

$$R_{eq} = (1\ k\Omega + 9\ k\Omega)\left(\frac{1.8V}{V_{in} - 1.8V}\right)$$

Equation 4: The equation for the equivalent resistance

$$V_{out} = \frac{1\ k\Omega + (1\ k\Omega + 9\ k\Omega)\left(\frac{1.8V}{V_{in} - 1.8V}\right)}{1\ k\Omega + (1\ k\Omega + 9\ k\Omega)\left(\frac{1.8V}{V_{in} - 1.8V}\right) + 9\ k\Omega} V_{in}$$

Equation 5: The equation for the output voltage of the voltage divider

Because the previous circuit caused a resistor to overheat, careful attention was paid to the power dissipated by the resistors of this circuit. While the manufacturer of the resistors was unknown, the resistors appeared to be standard 0.25 watt carbon film resistors. If a resistor overheated, it would need to be replaced by a high wattage power resistor.

To find the power dissipated by the resistors, first the current through them was found. At the maximum voltage of the stimulus (135 volts), the equivalent resistance of the diode would be

approximately 135 ohms (Equation 6). The output voltage would be approximately 15.12 volts (Equation 7). The current through the circuit would be 13.32 milliamps (Equation 8). The instantaneous power dissipated by the 9 kΩ resistor was greater the 0.25 watts (Equation 9). The instantaneous power dissipated by the 1 kΩ resistor was less the 0.25 watts (Equation 10). The instantaneous power dissipated by the light-emitting diode was 0.0240 watts (Equation 11).

$$R_{eq} = (1\ k\Omega + 9\ k\Omega)\left(\frac{1.8V}{135V - 1.8V}\right) = 135.\overline{135}\ Ohms$$

Equation 6: The equivalent resistance when the voltage generated by the inductor peaks at 135 volts

$$V_{out} = \frac{(1\ k\Omega + 135\ \Omega)}{(1\ k\Omega + 135\ \Omega) + 9\ k\Omega} 135V = 15.12\ Volts$$

Equation 7: The output of the voltage divider when the voltage generated by the inductor peaks at 135 volts

$$I = \frac{135V}{1\ k\Omega + 135\ \Omega + 9\ k\Omega} = 0.01332\ Amps = 13.32\ Milliamps$$

Equation 8: The current through the circuit when the voltage generated by the inductor peaks at 135 volts

$$P_1 = (V_1 - V_2)I = (135V - 15.12V)(0.01332A) = 1.597\ Watts$$

Equation 9: The instantaneous power dissipated by the 9 kΩ resistor when the voltage generated by the inductor peaks at 135 volts

$$P_2 = (V_2 - V_3)I = (15.12V - 1.8V)(0.01332A) = 0.1774\ Watts$$

Equation 10: The instantaneous power dissipated by the 1 kΩ resistor when the voltage generated by the inductor peaks at 135 volts

$$P_2 = (V_3 - V_4)I = (1.8V - 0V)(0.01332A) = 0.0240\ Watts$$

Equation 11: The instantaneous power dissipated by the light-emitting diode when the voltage generated by the inductor peaks at 135 volts

Since the wattage through the 9 kΩ resistor was greater than 0.25 watts, it was believed that the resistor would overheat. However, testing revealed the resistor would not overheat. In order to gain knowledge about what conditions can cause the resistor to overheat, several resistor specification sheets were consulted. The specification sheet for Vishay Standard Carbon Film Leaded Resistors contained several useful graphs showing what conditions cause their resistors to overheat [32]. The rated max wattage for their resistors was only valid at specific temperatures and durations. The rated wattage was only valid for temperatures less than 73 degrees Celsius [32]. For short duration pulses, the maximum wattage was higher. With pulses 1 millisecond in duration that occur at a rate of 1 hertz, the rated wattage was roughly 100 times greater [32]. This was likely true for the resistors used in the voltage divider, which explains why they did not overheat.

In order to reduce the heating of the resistors further, both the resistors in the voltage divider were scaled up by a factor of 10. Scaling both resistors by the same factor results in an output that is the same fraction of the input. With the new resistor values, the stimulus had a higher peak voltage, but a narrower width. This resulted in a weaker stimulus being felt by the arm. This was undesirable so the resistor values were reverted.

The stimulus waveform had a different shape when it was not connected to a test subject's body. For consistency, the waveforms were all recorded with a test subject's body connected. For testing purposes, it would useful to use an electrical circuit to simulate a test subject's body. It was believed that a test subject's body could be closely simulated with just a resistor and a capacitor in parallel. To determine suitable values for the resistor and capacitor, the shape of the stimulus was observed with the hand connected. Next, the hand was replaced with a resistor and a capacitor in parallel. The values of the resistor and capacitor was estimated based on previous measurements. Based on the shape of

the stimulus waveform, the values of the resistor and a capacitor were adjusted. This was repeated several times until the shape was comparable (Figure 30). The final resistance and capacitance values were 46 kiloohms and 25 nanofarads respectively.

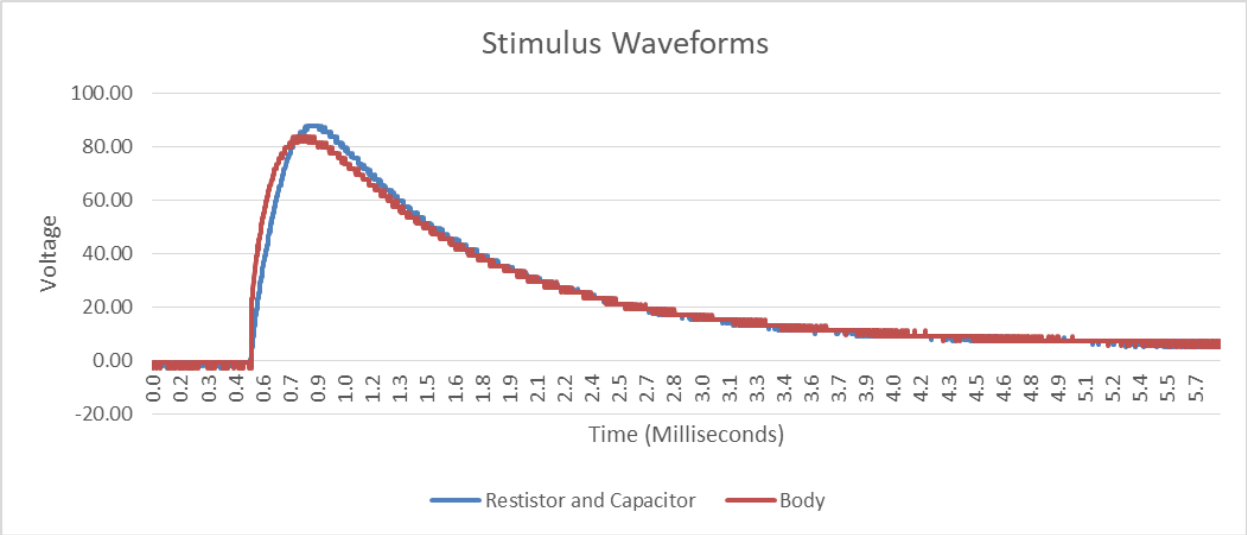

Figure 30: Graph of two stimulus waveforms. The red line is the shape of the stimulus when the stimulus circuit is connected to the body. The blue line is the shape of the stimulus when the stimulus circuit is connected to a resistor and a capacitor

Testing was performed to determine the amount of current traveling through the body. An 11 ohm resistor was placed in the stimulus circuit following the negative lead of the stimulating electrode (Figure 31). The peak voltage across the resistor was measured and used to calculate the peak current traveling through the body. The current through the body varied from 3.18 to 31.36 milliamps as the stimulus voltage was adjusted from 41.8 to 135 volts (Figure 32). These current values seemed reasonable for a stimulus circuit based on previous research studies.

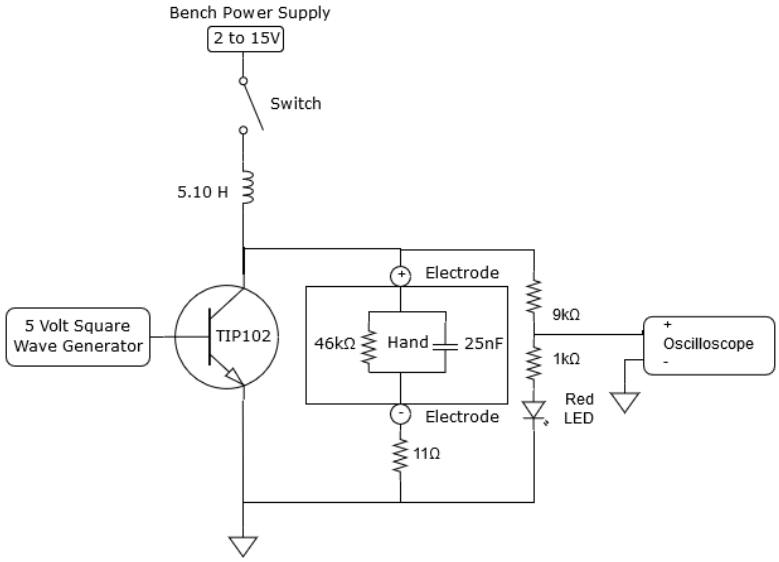

Figure 31: Diagram of the modified stimulus circuit. This circuit contains an additional 11 ohm resistor for measuring the current passing through the hand. The resistance and capacitance of the hand is represented by the 46 kiloohm resistor and the 25 nanofarad capacitor

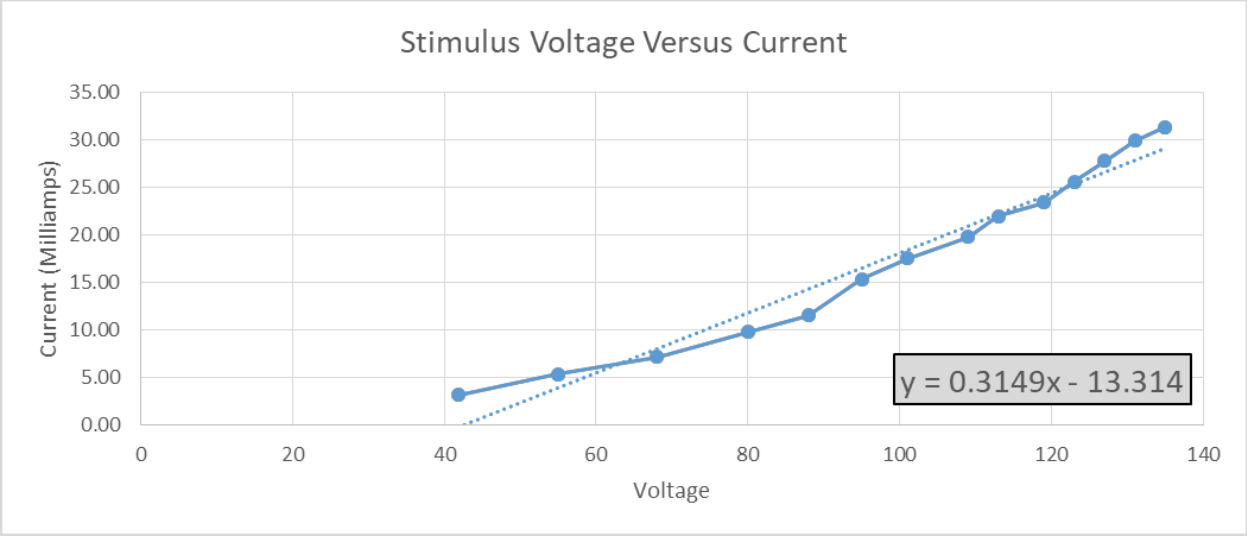

Figure 32: Graph of the peak current through the body based on the stimulus voltage used

3.11 Electrodes Used

Three types of electrodes were used with the stimulus and recording devices. The first was silver/silver chloride electrodes (Figure 33). Pediatric electrodes were used so that the electrode would easily fit on the hand. These electrodes had a gel adhesive and a foam back. These electrodes were used for observing signals in the body and sometimes, for stimulating.

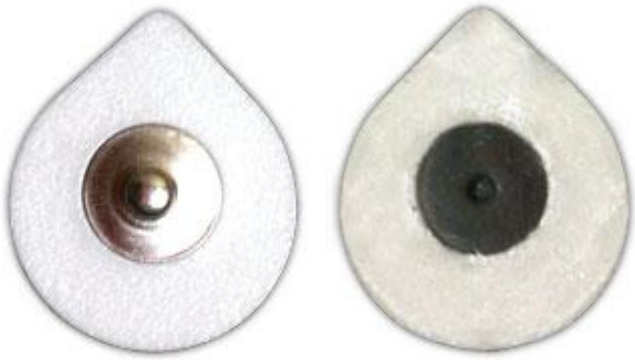

Figure 33: The top and bottem of the silver/silver chloride electrodes [33]

The second type of electrode was a stainless steel bar electrode (Figure 34). The bar electrode consisted of two circular stainless steel electrodes separated by one inch. The electrodes were concave, which meant that only their edges were in contact with the skin. Because of this, the surface area of the bar electrode was significantly less than the foam-gel electrodes. This electrode was used when stimulating at the wrist.

Figure 34: The stainless steel bar electrodes [34]

The third type of electrode was a stainless steel ring electrode (Figure 35). This electrode consisted of two loops made from a flexible coil of stainless steel. The loops could be tightened. This electrode was used when stimulating at the finger.

Figure 35: The stainless steel ring electrodes [35]

Because of the high voltages generated by the stimulus, both the bar and ring electrodes caused electrical burns in some cases. The occurrence of burns was reduced by coating the areas of the skin that contacted the electrode in electrolytic gel. It was further reduced by decreasing the stimulus voltage from approximately 110 volts to 95 volts.

This prevented burns when the arm was stimulated only a few hundred times. However, it did not prevent burns when the arm was stimulated 1000 times in a row. This may have occurred because the electrolytic gel was drying or because it was being pushed away from the electrode. The use of the ring and bar electrodes was discontinued due to the persistent burns. The foam-gel electrodes were used for both the recording and the stimulating electrodes.

3.12 Electromagnetic Noise Revisited

Increasing the stimulus voltage resulted in an increase in electromagnetic interference. In order to compensate for this, the stimulus and bio-amplifier were placed on different desks separated by a distance of 72 inches. The test subject sat between the two tables while connected to both the stimulus and the bio-amplifier. However, this did not remove the electromagnetic noise. Next, copper mesh was placed between the two tables and connected to earth ground in order to block electromagnetic interference traveling through the air. However, this was not effective at blocking the electromagnetic interference.

Although completely blocking the electromagnetic interference between the two devices was impossible, it was likely possible that the interference could be reduced to the point where it would no longer disrupt the nerve signals. It would no longer disrupt the nerve signals because there would be some delay, known as onset latency, before the nerve signals began to appear. The onset latency is

between 1.8 to 3.6 milliseconds for sensory nerve signals when measured from the wrist to the second or third digits [30]. It is between 3.0 to 4.6 milliseconds for motor nerve signals when measured from the wrist to the abductor pollicis brevis [30]. Lastly, it is between 2.7 to 5.1 milliseconds for motor nerve signals when measured from the wrist to the second Lumbrical [30]. As long as the electromagnetic interference did not last for more than 1.8 milliseconds, it will not prevent recording of these nerve signals.

The first step to reduce the electromagnetic interference was reducing the stimulus duration. It was possible for two stimuli generated from the same input voltage to have different durations because of added components in the stimulus circuit (Figure 36). Resistors and capacitors had been added to the stimulus circuit to change the shape of the stimulus. These components had the unintended effect of increasing the stimulus duration. However, having the correct duration was more important than having the right shape for the stimulus. Therefore, all added resistors and capacitors were removed from the stimulus circuit. However, the stimulus continued to have a long trailing edge even with the extra components removed.

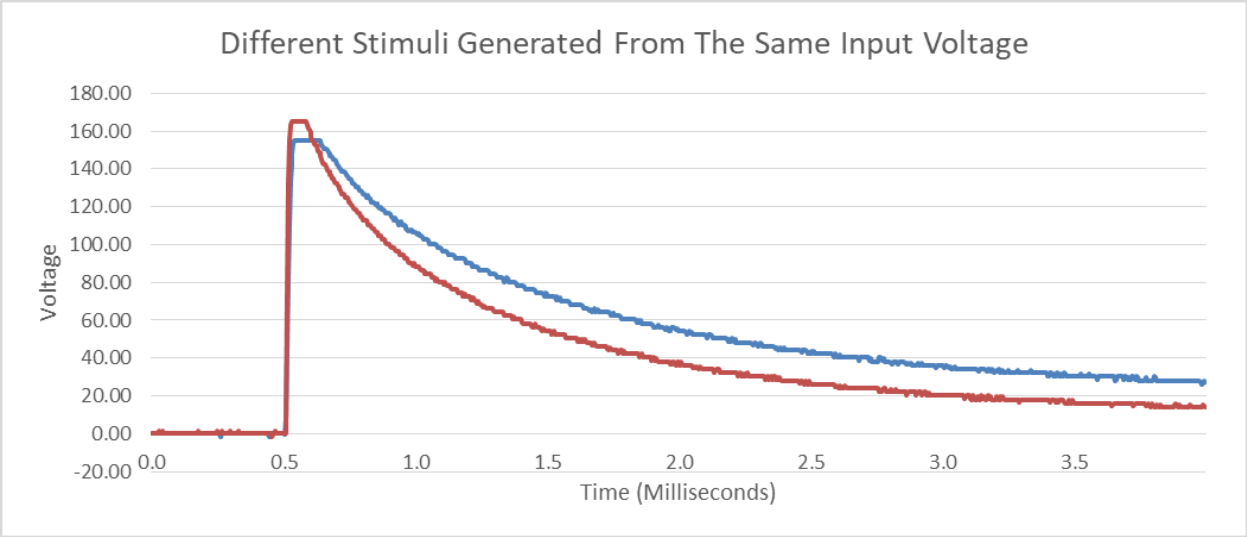

Figure 36: Two stimulus waveforms generated from the same input voltage. The blue waveform has a longer duration because stimulus circuit that generated it had added components

Removing the extra components reduced the stimulus width to approximately 0.5 milliseconds. This duration was short enough that the stimulus should not interfere with viewing the nerve signal. However, it was possible that a 0.5 milliseconds stimulus would cause more than 0.5 milliseconds of electromagnetic interference.

3.13 Bench Amplifier

The bio-amplifier was compared to a regular bench amplifier in order to assess the quality of its output. The bench amplifier it was compared to was an EG&G PARC Model 113 pre-amplifier. This amplifier could filter signals. It had 11 different low-pass filter values and 11 different high-pass filter values. The bio-amplifier had a high-pass filter cutoff of 20 hertz and a low-pass filter cutoff of 2000 hertz. The bench amplifier did not have 20 hertz as a high-pass filter value, so the high-pass cutoff was set to 10 hertz instead. It did not have 2000 hertz as a low-pass cutoff frequency, so the low-pass cutoff was set to 3000 hertz. Lastly, the bio-amplifier could amplify signals by 30,000 times. The bench amplifier could not amplify by 30,000 times, so its amplification was set to 10,000 times, which was its maximum

amplification level. While there were differences between the settings of the bio-amplifier and the bench amplifier, doing a comparison of the two should provide useful information.

The comparison of the bio-amplifier to the bench amplifier was performed by using the same input with both amplifiers and observing the outputs. A Bio-Tek ECGplus handheld waveform generator was used as the input. This device was set to output a cardio signal, which was recorded (Figure 37). In order to compare the output of the handheld waveform generator and each of the two amplifiers, the output of the handheld waveform generator was filtered. This was accomplished by changing the oscilloscope input from DC to AC coupled (Figure 38).

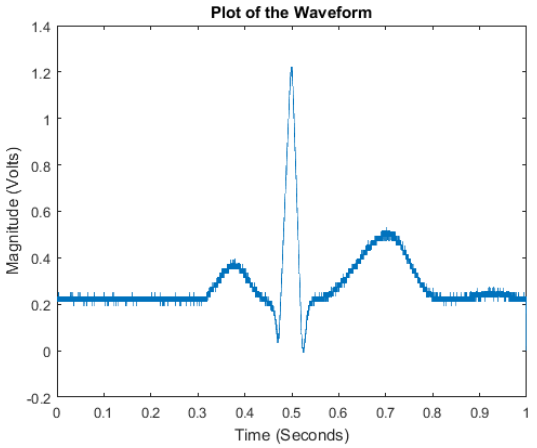

Figure 37: The output of the Bio-Tek ECGplus handheld waveform generator

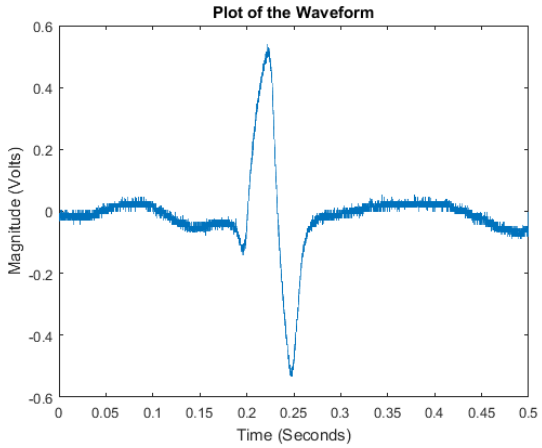

Figure 38: The output of the Bio-Tek ECGplus handheld waveform generator after being AC coupled

The output of both amplifiers was closer to each other than expected. The bench amplifier had some 60-hertz noise (Figure 39). The output of the bio-amplifier contain some random noise (Figure 40). The distortion caused by the random noise in the bio-amplifier output was worse because it distorted the peaks of the signal more. For this reason, the bench amplifier was used to continue searching for a nerve impulse signal.

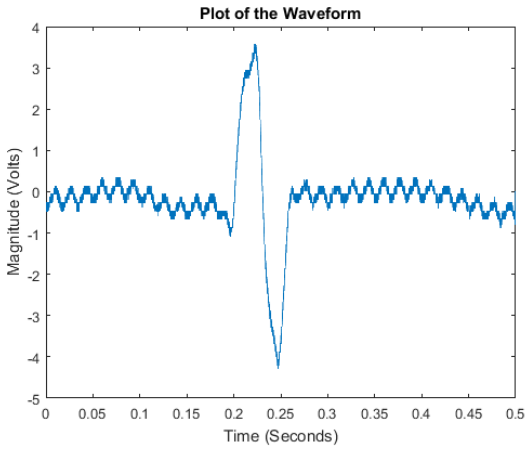

Figure 39: The output of the bench amplifier

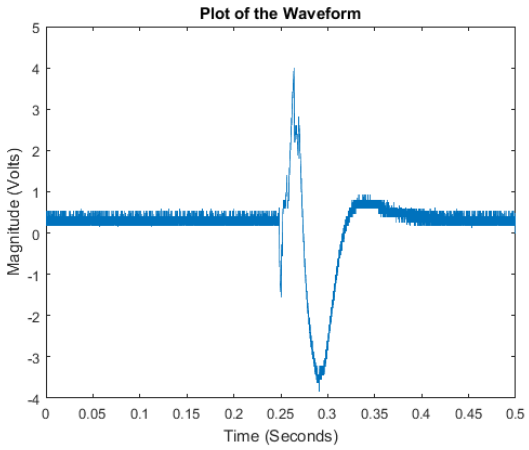

Figure 40: The output of the bio-amplifier

3.14 Bench Amplifier Isolation

However, the bench amplifier did not have an isolation stage. Because of this, the stimulus was jumping to the bench amplifier input leads, which was hazardous and interfered with recordings. The stimulus jumping between the two pairs of leads was felt by the test subject. The recorded signals from the arm were also distorted. An isolation stage needed to be added between the test subject and the bench amplifier to protect the test subject and prevent distortion. This isolation stage would require three lines because the bench amplifier was using three lines to take differential recordings of the body.

One ISO 124P integrated circuit was used to isolate each line. Adding an isolation stage successfully stopped the stimulus from being grounded to the bench amplifier. However, it also added a small amount of random noise. The amount of added noise was measured by comparing the input of the isolation stage to its output (Figures 41 and 42). The output had a smaller amplitude than the input so it was scaled up (Figure 43). The amount that the output was scaled was determined by comparing the average amplitude of all the points in the central peak. After the output was scaled, the input was

subtracted from it to calculate the noise (Figure 44). The signal-to-noise ratio of the input to the estimated noise was 11.2742 decibels.

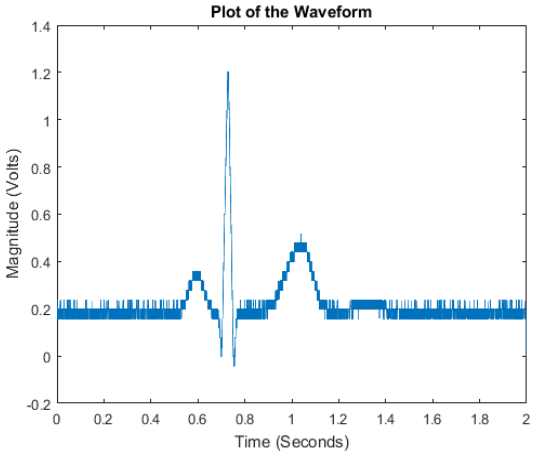

Figure 41: The input to the isolation stage

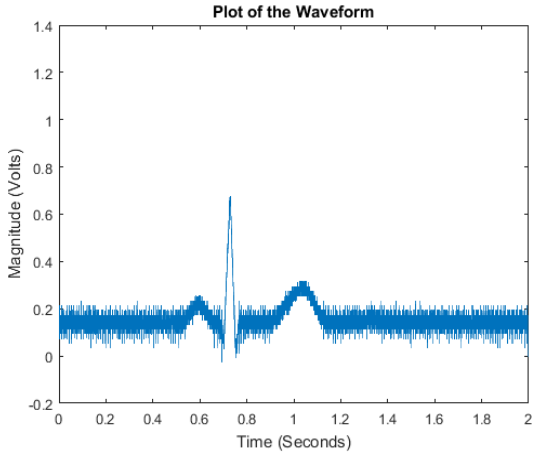

Figure 42: The output of the isolation stage

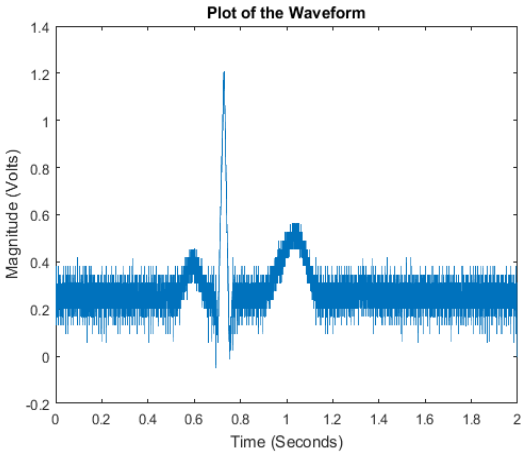

Figure 43: The scaled output of the isolation stage

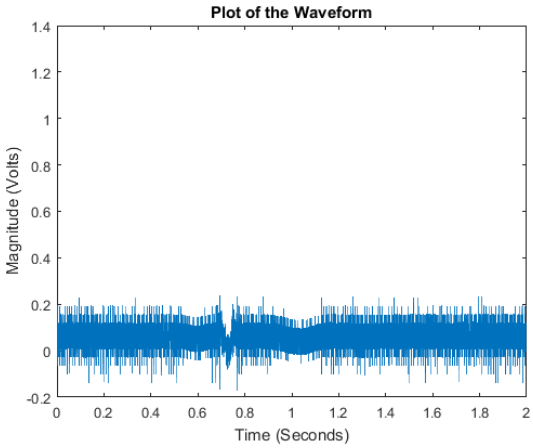

Figure 44: The estimated noise added by the isolation stage

The cardio signal used for the previous test had a peak voltage of about 1.2 volts. However, an actual motor nerve signal should be approximately 12 millivolts. So the previous test was performed with the input signal reduced by a factor of 100 (Figure 45). In this case, the noise in the output was larger than the input signals peak (Figure 46). Because of this, it was hard to determine whether the peak was the same size as the input or whether it needed to be amplified.

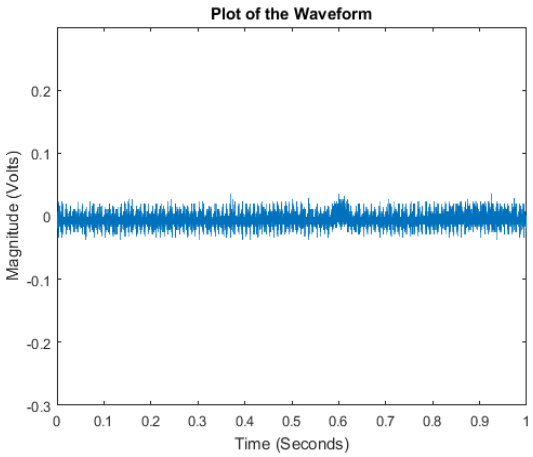

Figure 45: The input to the isolation stage

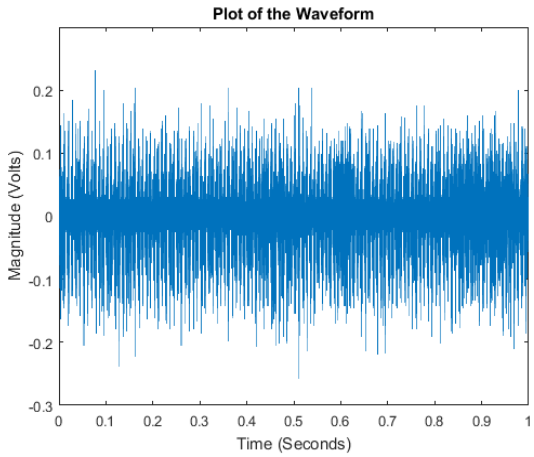

Figure 46: The output of the isolation stage

In this case, the output was scaled down (Figure 47). The amount that the output was scaled down was determined by comparing the average amplitude of specific areas in both plots. This scaling was less precise because the noise was larger than the peak of the input signal. After the output was scaled, the input was subtracted from it to determine the noise (Figure 48). The signal-to-noise ratio of the input to the estimated noise was -10.4871 decibels. Because the scaling was not precise, this estimation of noise was also not precise.

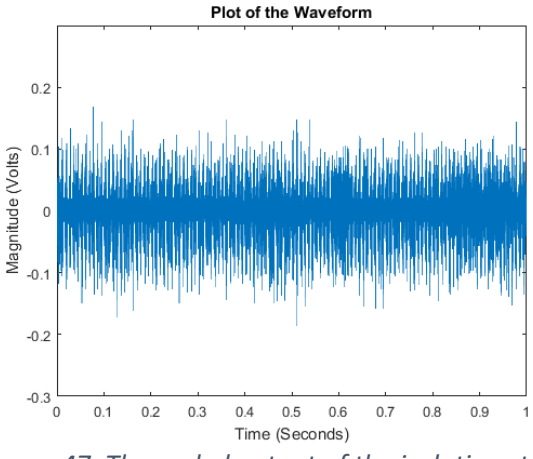

Figure 47: The scaled output of the isolation stage

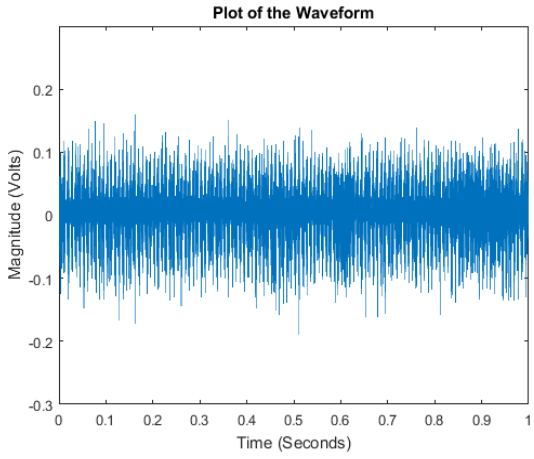

Figure 48: The estimated noise added by the isolation stage

Although the amplitude of the noise was only a fraction of a volt, it was still enough to make viewing an action potential difficult or even impossible. The isolation circuit increased the noise likely because the breadboard and wires it was built from were not shielded enough. Covering the entire circuit with aluminum foil in order to block out some of the noise was considered. However, it was decided that it would be more effective to remove the isolation circuit altogether and isolate the test subject another way.

3.15 Battery-Based Power Supply

Another way to isolate the test subject from earth ground tested that was tested was to power the amplifier and the oscilloscope off a battery. The battery used was a Cyber Power CP1350PFCLCD uninterruptable power supply used for keeping computers running during short power outages. The power supply battery had a seven amp-hour capacity and was capable of running both the oscilloscope and the amplifier for one hour on a single charge.

The uninterruptable power supply was used without plugging in the power cord because this would break isolation. This had the unintended consequence of causing the signal on the oscilloscope to have a DC offset. The DC offset cause the signal to jump from around 27.5 volts to -22 volts (Figures 49 and 50). When the offset was negative, the signal was also inverted. To account for this, the saved data underwent additional processing before it was graphed. If the signal was positive, it was shifted until the average of all its values was 0 volts (Figure 51). If the signal had a negative DC offset, it was inverted and shifted by the average of all its values (Figure 52).

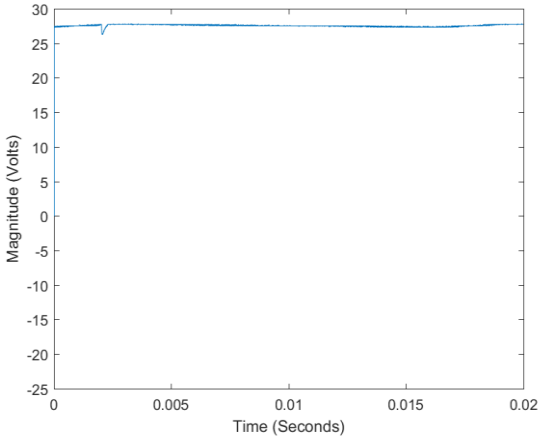

Figure 49: A signal with a positive offset

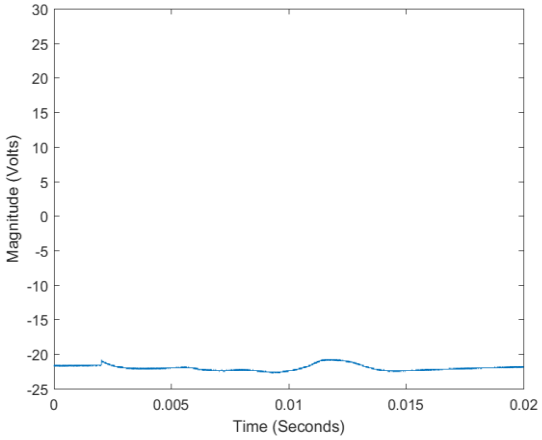

Figure 50: An inverted signal with a negative offset

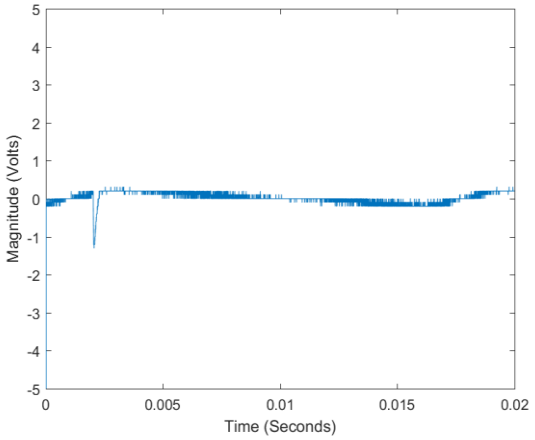

Figure 51: Shifted version of the signal with the positive offset

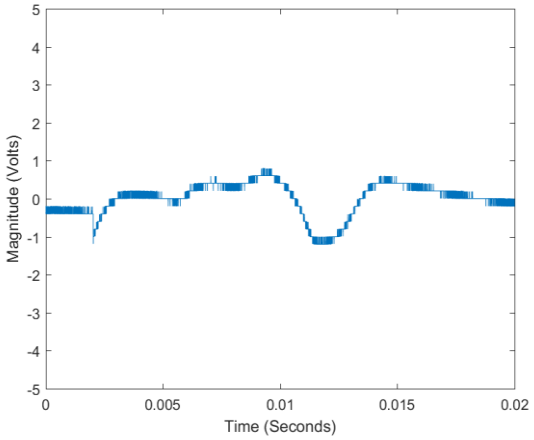

Figure 52: Shifted and inverted version of the signal with the negative offset

The uninterruptable power supply provided sufficient power while isolating the oscilloscope and the amplifier from earth ground. It also significantly reduced noise when compared to the separate isolation circuit. The stimulus circuit was not powered by the battery backup because it would not reduce the noise in the recording from body.

3.16 Testing for Motor Nerve Signals

Using a battery-based power supply reduced the noise in the recordings enough to observe a signal coming from body. This signal was observed when stimulating the median nerve at the wrist and recording at the base of the thumb.

The Manual of Nerve Conduction Studies was consulted for information about electrode placement [30]. The positive and negative stimulating electrodes were placed below the crease of the wrist (Figure 53). They were placed an inch apart with the negative electrode being closer to the wrist. The positive and negative recording electrodes were placed on the abductor pollicis brevis. They were placed an inch apart with the negative electrode was placed closer to the thumb. The ground recording electrode was placed in the center of the back of the hand.

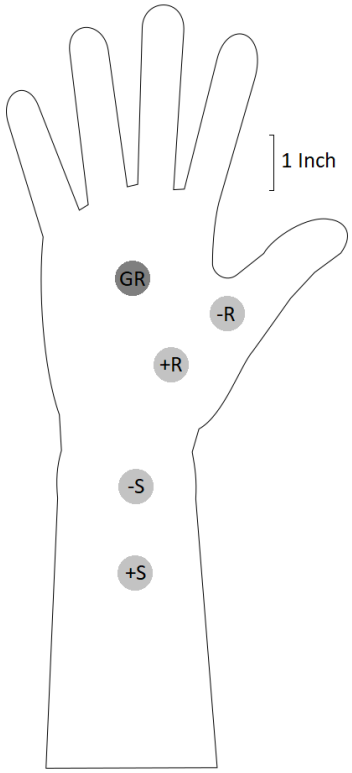

Figure 53: The placement of electrodes on the hand. The "–R" symbol represents the negative recording electrode. The "+R" symbol represents the positive recording electrode. The "GR" symbol represents the

ground recording electrode. The "–S" symbol represents the negative stimulating electrode. The "+S" symbol represents the positive stimulating electrode

The first major peak of the signal occurred about 6.5 milliseconds after stimulation (Figure 54). It had a peak-to-peak amplitude of about 2 volts when the amplifier gain was set to 10,000. Thus, the amplitude of the signal was around 200 microvolts. A motor nerve signal would be expected to occur around 3.0 to 4.6 milliseconds after stimulation and have an amplitude of about 10.2 millivolts [30]. So additional testing was performed to determine if this peak was actually a nerve signal.

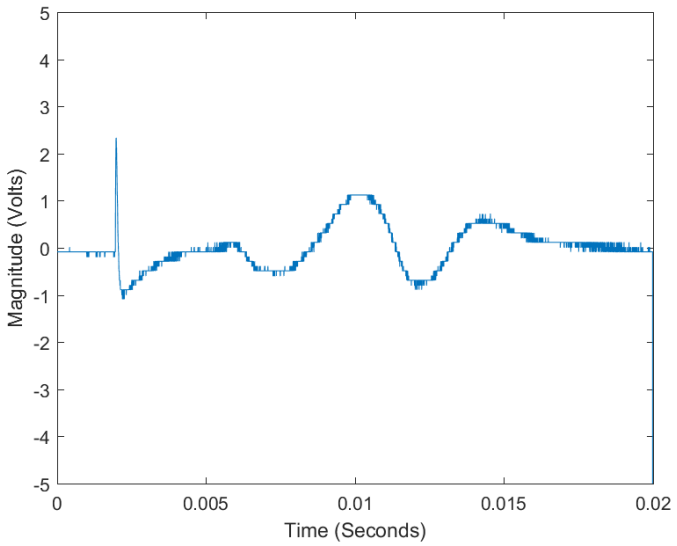

Figure 54: Response recorded from the thumb after stimulating the median nerve at the wrist

By moving the stimulating electrodes slightly, whether or not the thumb twitched could be controlled. When the thumb was not twitching, the signal disappeared. This evidence suggested that the peak being observed was caused by a muscle activation, not by a nerve signal.

To investigate this further, a new set of tests was performed at a location where a muscle signal would be unlikely to show up. Stimulations were performed on the middle finger and the signals from the median nerve of the wrist were recorded. When recording at the wrist, no peaks in the signal were

visible (Figure 55). This information supported the position that the signal observed before was a muscle activation.

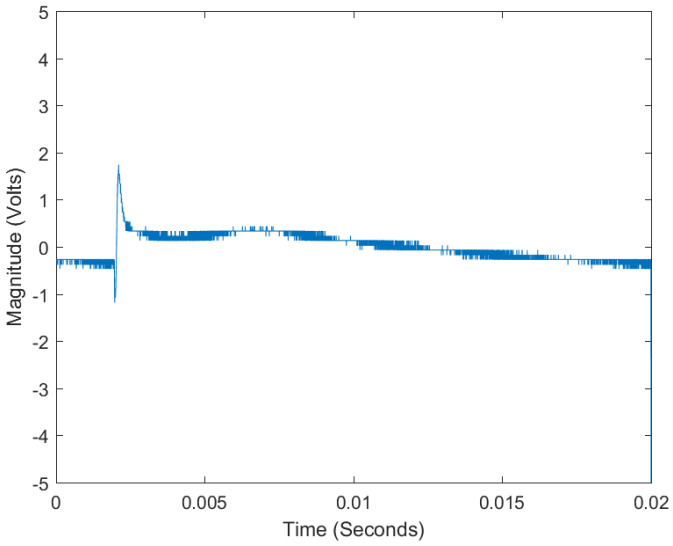

Figure 55: Response recorded from the median nerve of the wrist after stimulating the middle finger

3.17 Final Attempts to Observe a Nerve Signal

It was theorized that the nerve signal might be very small and hard to see. Signals from the body were amplified beyond 10,000 times by adding an instrumentation amplifier before the bench amplifier. However, the addition circuitry of the instrumentation amplifier added significant 60-hertz noise to the signals.

The tests were repeated in faraday cage to reduce the amount of noise added. The faraday cage was approximately 4 ft. x 8 ft. x 8 ft. in size and could fit the test subject and all the equipment comfortably. The faraday cage was made from a fine copper mesh. The mesh was connected to earth ground. However, even inside the faraday cage, no nerve signals were visible.

The instrumentation was removed because it added significant 60-hertz noise to the signals. Instead, a second bench amplifier was added in series with the first bench amplifier. This second bench amplifier did not add significant noise. However, even with the low noise and high gain output of the second bench amplifier, no nerve signal was visible.

This was the final attempt to amplify and observe an action potential traveling along a nerve axon. At this point, development of the simpler nerve conduction device was halted and development of the second nerve-testing device began. The bio-amplifier circuit was not used after this point. The stimulus circuit continued to be used and developed with the new testing device.

3.18 Thumb Twitch Testing System

Because a nerve signal had yet to be observed at this point, it was decided to find another way of testing nerve health other than observing the nerve signals directly. The alternate test selected was to stimulate the thumb to twitch and measure the delay between the stimulus and the thumb moving. If the nerve was damaged or diseased, it was theorized the thumb would react slower.

To measure the reaction time of the thumb, a movement sensing circuit was built from a speaker and an infinite gain amplifier (Figure 56). The finger to be tested was placed on center of the speaker. When the finger moved the speaker would generate a small voltage potential. That voltage potential was amplified into a higher voltage DC signal by the infinite gain amplifier. The peak from the stimulus and the output from the movement sensing circuit could be observed together on an oscilloscope to determine how long the thumb took to twitch (Figure 57).

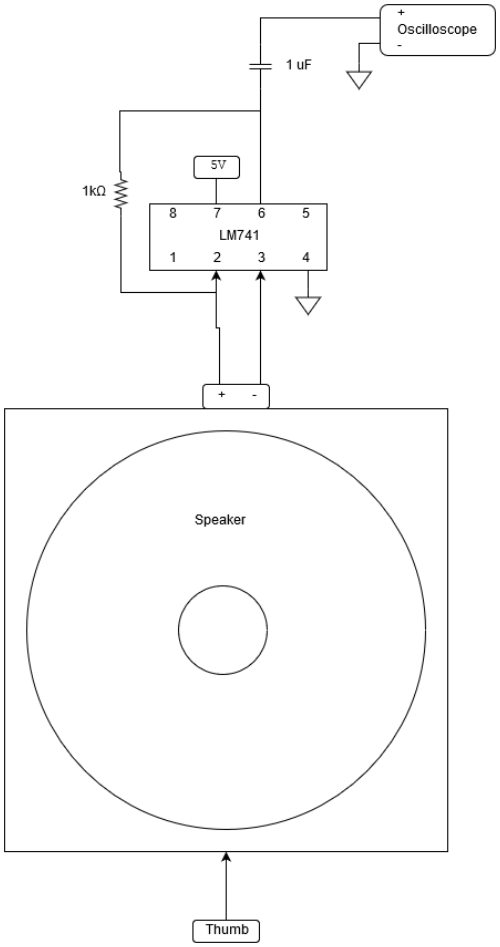

Figure 56: Thumb movement sensing circuit

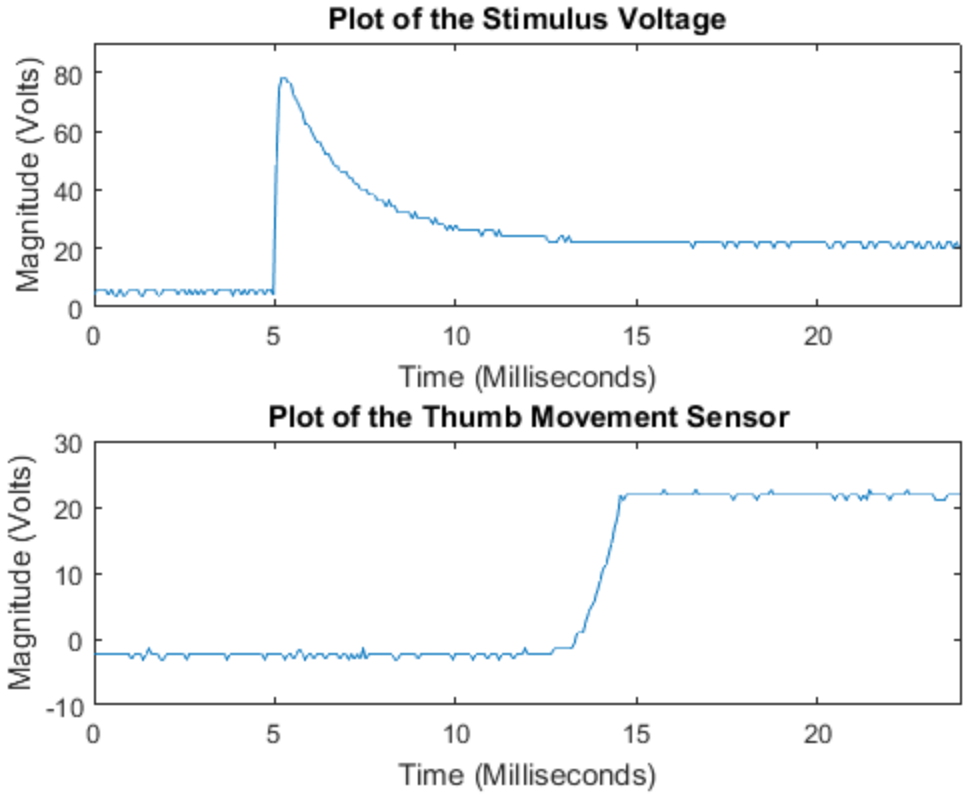

Figure 57: Plot of the stimulus voltage and the output of the thumb movement sensor. This shows the time difference between the nerve being stimulated and the thumb moving

The speaker used was 50 millimeters in diameter and had 8 ohms of impedance. It was very sensitive to movement. The exact sensitivity of the speaker could not be determined. However, the distance the thumb moved when stimulated was always more than enough for it to detect.

Initial tests showed the response time of thumb after being stimulated was around 75 milliseconds. This measurement was obviously too high. After some investigation, it was determined that the thumb movement sensor was not activating when the muscles of the thumb contracted, but when they relaxed. This was caused by the positive and negative leads from the speaker being connected to the wrong pins of the infinite gain amplifier. This was easily fixed by swappping the speaker wires to the opposite input pins.

3.19 Microcontroller-Based System

This system was made more compact and portable by using an Arduino UNO microcontroller board to control the stimulus and automatically record the twitch times. Initially, 9-volt batteries were used to power both the stimulus and the movement sensing circuit instead of a bench power supply. In order to save batteries and keep test results consistent, a 9-volt bench supply was later used to power the stimulus. The movement sensing circuit was later powered by the 5-volt supply on the Arduino UNO (Figure 58).

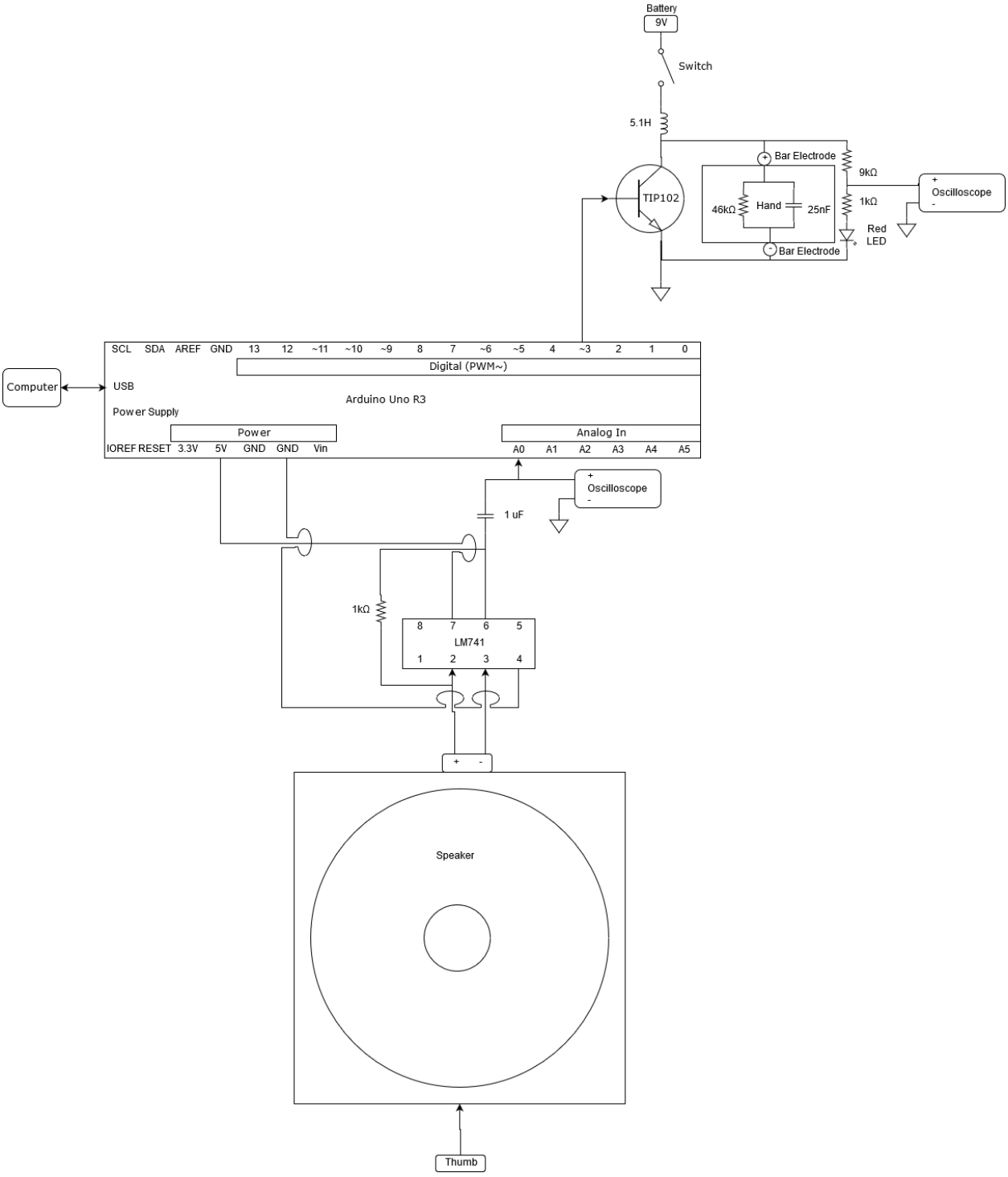

Figure 58: The full stimulus and thumb movement sensing system. The resistance and capacitance of the hand is represented by the 46 kiloohm resistor and the 25 nanofarad capacitor

Initially, the stimulus circuit was connected to thirteenth digital output pin of the Arduino UNO board. However, the connection was moved to the third digital pin after it was realized that the thirteenth pin rapidly turns on and off three times when the Arduino UNO starts up. The pin turning off and on was causing the stimulus to activate unnecessarily.

The Arduino UNO board was controlled by a custom program (Appendix: Program 7). This program controlled both the activation of the stimulus, and monitored of the thumb twitch sensor. It recorded the time delay between the stimulus activating and the thumb twitching. It would perform 100 tests at a time and then analyze the data from the tests. The sum, average, and standard deviation of the set of data was calculated during the analysis. The data from each set of tests was saved in a spreadsheet.

The stimulus circuit generated a weaker stimulus when controlled by the Arduino UNO board (Figure 59). The peak voltage of the Arduino UNO-based stimulus was 16.8% lower on average.

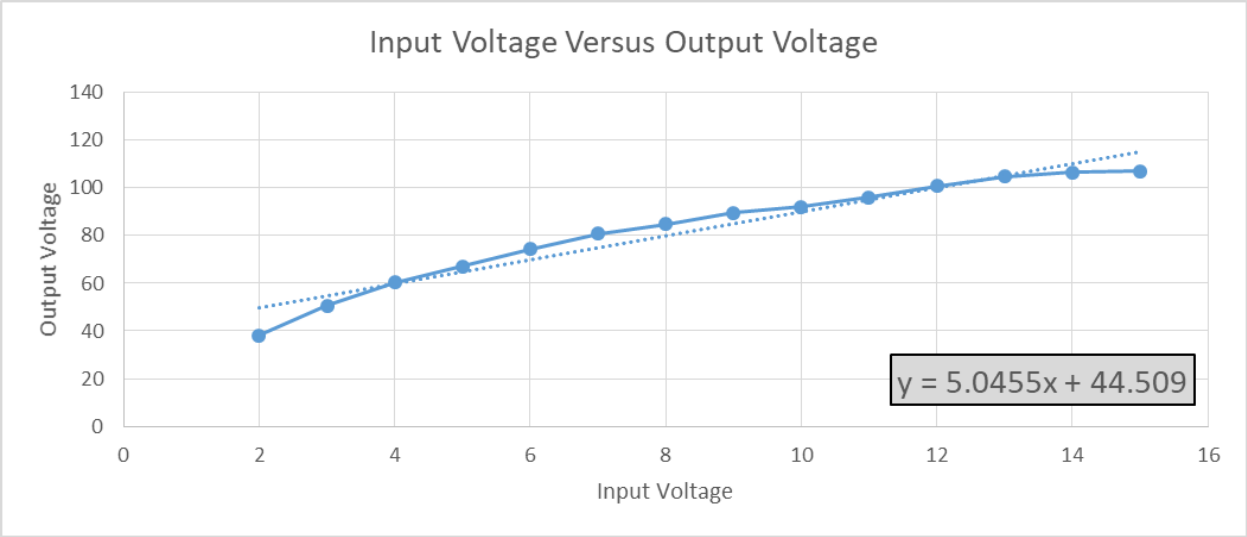

Figure 59: Graph of the input voltage versus the output voltage for the Arduino UNO-based stimulus

Stimulation was performed on the median nerve about 3/4 of an inch to 1 inch below the crease of the wrist (Figure 60).

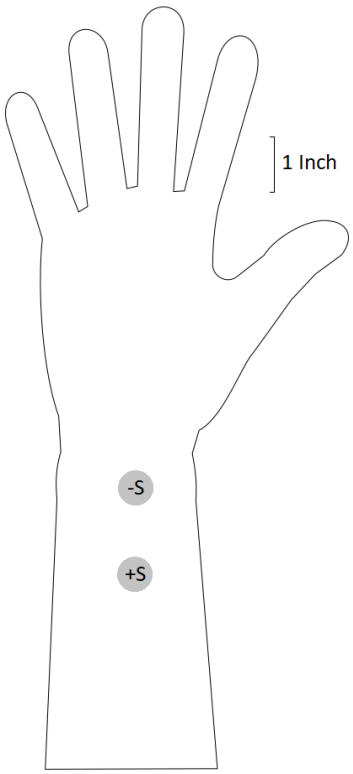

Figure 60: The placement of electrodes on the hand. The "–S" symbol represents the negative stimulating electrode. The "+S" symbol represents the positive stimulating electrode

The accuracy of the time measurements taken by the Arduino UNO board was tested by comparing the measurement made by Arduino UNO to measurements made by an oscilloscope. During the test, the stimulus was not connected to the body. Instead, the thumb movement sensor would be manually pressed sometime after the stimulus activated. The signals from the stimulus and the thumb movement senor were sent to oscilloscope. Just the signal from thumb movement sensor was sent to the Arduino UNO since it controlled the activation of stimulus. Using the time measurement tools on the oscilloscope, the delay time between the two signals was measured manually. This measurement was compared to the automatic measurement made by the Arduino UNO. Ten tests were performed and the results were averaged. There was a 1.4% average error in the Arduino UNO measurements when compared to the oscilloscope measurements. This amount of error was considered insignificant. Such a

small amount of error could have been caused by a user error when manually measuring the delay times on the oscilloscope.

3.20 System Precision

Initial tests showed the time delay between the stimulation of the median nerve and the thumb twitching to be around 9 to 11 milliseconds. More tests were needed to determine how different factors affected the response time of the thumb. For these tests to be conclusive, the time delay measurements of the Arduino UNO board would need to precise and accurate.

Analysis of several sets of tests was done to determine the minimum time difference between samples. The Arduino website says the sample rate for the UNO board should be about 10,000 samples per second or 100 microsecond per sample [36]. The measured minimum time between samples was 112 microseconds. This means it is sampling at roughly 8,929 samples per second. Since the delay times are around 10 milliseconds, the sampling rate is about 1% of a standard measurement.

Control tests were performed where nothing was changed between tests in order to determine the precision of the delay measurements. Five sets of 100 control tests were analyzed (Figures 61 to 65). The average standard deviation of measurements within each group of 100 tests was about 0.77 milliseconds. The standard deviation between the five sets of tests was about 0.35 milliseconds. The average twitch delay time of the five sets was 9.60 milliseconds. The intragroup precision was about 8.0% of an average measurement, and the intergroup precision was about 3.6% of an average measurement.

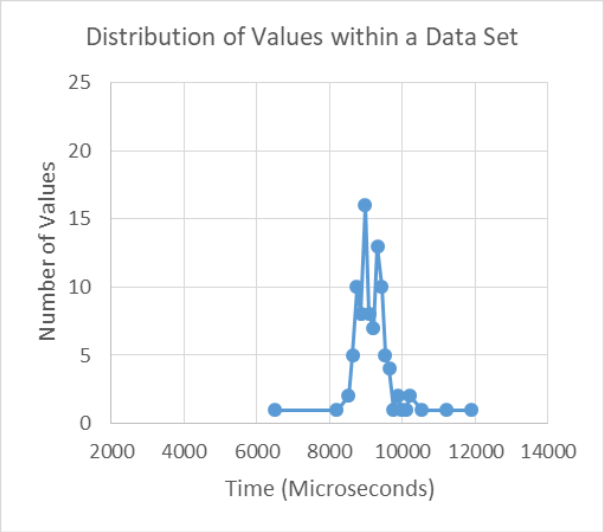

Figure 61: Distribution of 100 measurement from the same set. The standard deviation is 589 microseconds

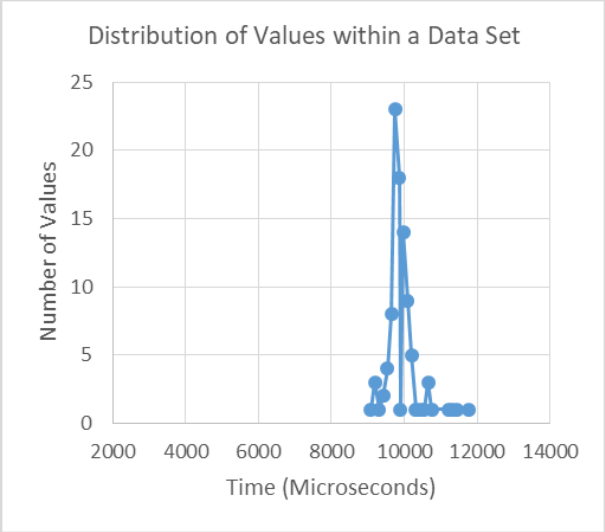

Figure 62: Distribution of 100 measurement from the same set. The standard deviation is 429 microseconds

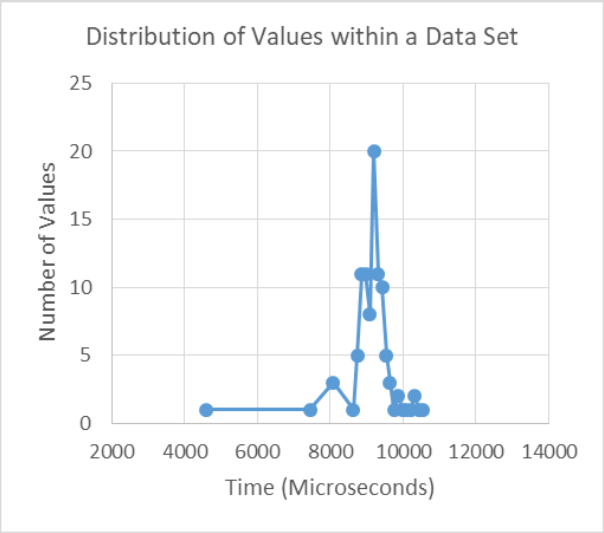

Figure 63: Distribution of 100 measurement from the same set. The standard deviation is 654 microseconds

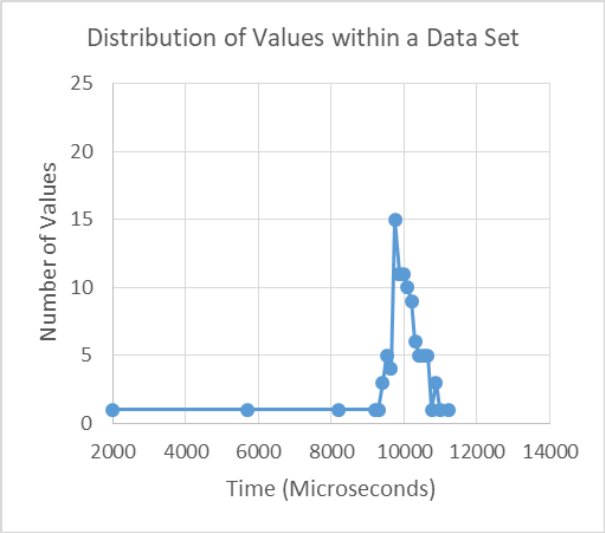

Figure 64: Distribution of 100 measurement from the same set. The standard deviation is 1008 microseconds

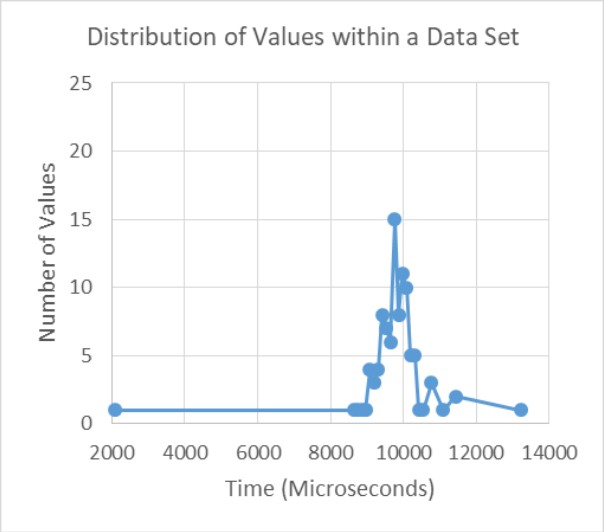

Figure 65: Distribution of 100 measurement from the same set. The standard deviation is 981 microseconds

Analysis of several sets of measurements was done to determine if there was a significant change in response time after each measurement. Potentially, there could be a slow increase or decrease in the response time of a digit after repeated testing. Ten sets of 100 measurements were analyzed. The average increase after each median nerve test was about 2.62 microseconds. The average increase after each ulnar nerve test was about 2.51 microseconds. However, more extensive testing is required to confirm these results.

3.21 Simulating Nerve Compression

This ability of this device to detect peripheral nervous disorders was based on the principle that peripheral nervous disorders cause the velocity of nerve signals to decrease. The time delay between the stimulation and the thumb twitch should increase slightly if the median nerve of the test subject is affected by a peripheral nerve disorder. This research did not have access to a person with a peripheral nervous disorder. Instead, a peripheral nervous disorder was simulated by using different methods to

slow down the nerve signals of healthy person. Whether or not these methods would actually be effective at slowing down nerve signals was unknown.

In an attempt to simulate nerve compression, two different methods of changing the nerve signal velocity were proposed and tested. The first method was exercising the thumb with handgrip exercisers (Figures 66 and 67). It was theorized that repeatedly using the thumb might cause the nerves signals traveling to the thumb muscles to slow down. The second method was compressing the ventral side of the wrist just before the wrist crease in order to pressurize the carpal tunnel. This method was considered a provocative test. It was theorized that this might cause similar effects as a compression-based medical condition such as carpal tunnel syndrome.

Whether Arduino UNO device sampled fast enough or was precise enough would depend on how much these methods of changing the nerve signal velocity caused the thumb movement delay to change. If a method caused no change in the measured delay then that method is either not effective at simulating nerve damage or the measurement system is not precise enough to measure the change.

The exercise tests were performed with two different types of hand exercisers. The first used a thick metal coil to provide resistance (Figure 66) and the second used elastic bands to provide resistance (Figure 67). Three elastics, which each exerted a force of about three foot-pounds, were used with elastic-based exerciser. Each set of tests only used a signal exercise device. However, not every set used the same device. This may have added some variance to the test results.

Figure 66: The metal coil-based hand exerciser used

Figure 67: The elastic-based hand exerciser used

Four sets of exercise tests and two sets of control tests were performed using the median nerve. Both exercise devices here held in a way that targeted the thumb muscles. The metal coil-based device was held upside down so the thumb was pressing against the end of the handle. Likewise, when the elastic band exerciser was used, the hand was positioned so the thumb was primarily exercised. During each set of exercise tests, a certain number of repetitions would be performed with the exercise device before the thumb twitch delay measurements were recorded. The number of exercise repetitions performed was 20 in two sets of tests, 50 in one sets of tests, and 100 in all other sets of tests. The number of delay measurements taken between sets of exercises was 100 in three sets of tests and 500 in one set of tests. The average delay of each set of tests was saved in a spreadsheet.

For comparison, two sets of thumb twitch delay measurements was taken without having performed any exercises. During each of the two control tests, five sets of 100 measurements were taken. The hand

was not exercised between sets of tests. The average delay of each set of tests was saved in a spreadsheet.

Exercise tests were also performed using the ulnar nerve. These tests were performed using only the elastic hand exerciser. The hand was positioned so that all the fingers except the thumb were exercised. One control test and two exercise tests were performed with the ulnar nerve. Twenty exercise repetitions were performed between each set of measurements in the exercise tests. Because the ulnar nerve innervates the little finger, measurement were taken using the little finger instead of the thumb. The electrodes were placed on the ulnar nerve and 3/4 of an inch below the wrist (Figure 68). The electrodes had to be positioned very carefully on the arm because they needed to be directly above the ulnar nerve. Slight movement of the electrodes to the left or right, would cause the little finger to stop twitching. The stimulating the ulnar nerve required more precise placement of the electrodes than stimulating the median nerve required. The first reading was taken without having performed any exercises. One hundred twitch delay measurements taken between sets of exercises. The average delay of each set of tests was saved in a spreadsheet.

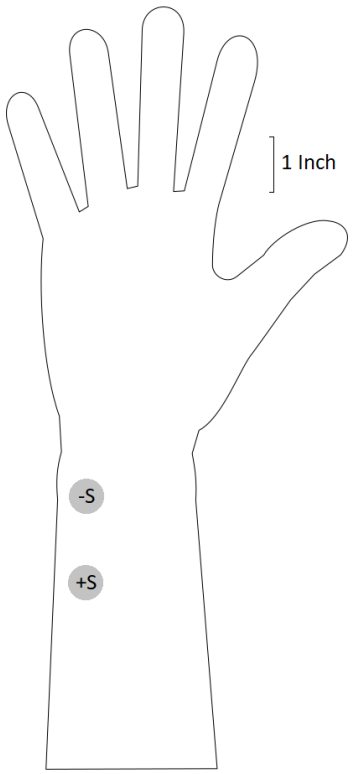

Figure 68: The placement of electrodes on the hand. The "–S" symbol represents the negative stimulating electrode. The "+S" symbol represents the positive stimulating electrode

Several different methods of compressing the median nerve were tested to see if they had any measurable effect on the response time of the thumb. The median nerve was compressed by bending the wrist, pressing on it with the other hand, putting a metal weight on it, and wrapping the wrist with tape. The metal weight was placed on the nerve using a metal stand that allowed a weight plate to compress a small area (Figure 69). Measurements of the thumbs response time were taken before, during, and after the nerve was compressed. Compression of the median nerve was performed for either 5 or 10 minutes. The average delay of each set of tests was saved in a spreadsheet.

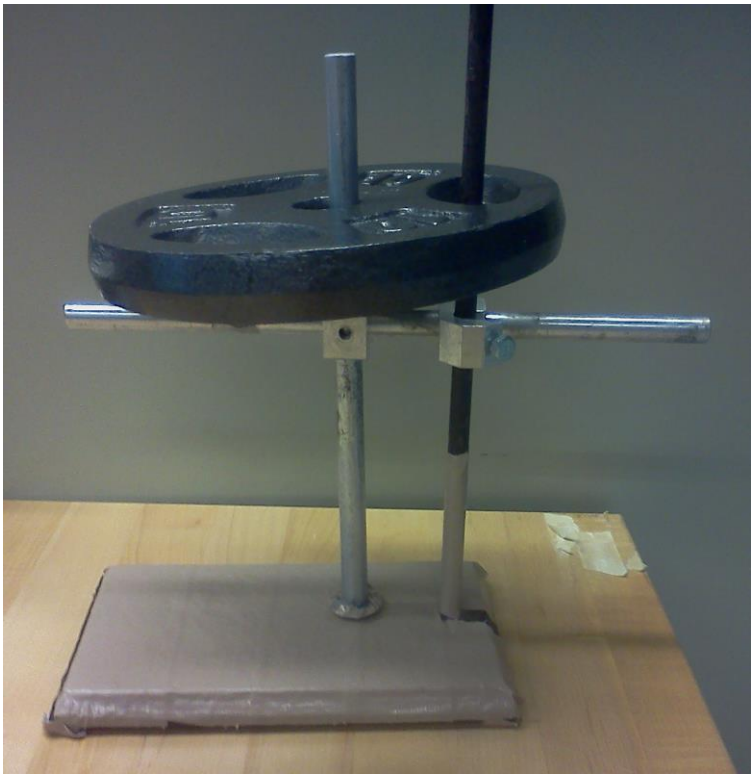

Figure 69: The device used to apply weight to a small area

A compression test was also performed on the ulnar nerve. Four control measurements were recorded with no weight on the wrist. Then a weight was placed on the wrist and measurements were taken every 5 minutes for 25 minutes. Thirty minutes after the compression was completed, three more control tests were performed. The average delay of each set of tests was saved in a spreadsheet.

All the saved data was analyzed to determine if compression or exercise had any effect on the response time of the thumb or little finger. Overall, the data was inconclusive. Most compression and exercise tests did not have delay times significantly longer or shorter than the control tests. Those that did were retested and had insignificant results in the later tests. No method of compression or exercise consistently caused delay times significantly longer or shorter than the delay times in the control tests.

A test was performed to determine how much moving the stimulus further from the thumb would affect the response time of the thumb. The response time increased by roughly 0.2 milliseconds every quarter inch the electrodes were moved. However, there was enough variance between the measurements that additional testing is required to confirm this result.

Moving both the electrodes slightly off to the side of the median nerve made it harder to stimulate it. This was especially noticeable when stimulating the ulnar nerve.

4. SUMMARY OF THE RESULTS

The overall goal of building a simple electronic device to assess nerve health was never reached. However, several design goals were reached. Many different experiments were performed in order to reach these goals. In some cases, these experiment lead to the goals being adjusted.

The initial goal for the stimulus was for it to generate a waveform that peaked at 120 volts. This voltage level was selected as the goal because it was believed that a voltage that high would be necessary to evoke an action potential in the median nerve using surface electrodes. In order to confirm that a low-voltage stimulus would not work, several different low-voltage stimulus circuit designs were built before a working high-voltage design was created. None of the low-voltage stimuli were able to cause a noticeable motor response. A high-voltage stimulus circuit was created by using a 5.1 henry inductor. The fact that this stimulus would cause fingers to twitch proved that it was effective at causing nerves to generate motor action potentials. This circuit was the only stimulus that could cause motor responses using the median or ulnar nerves.

The stimulus circuit could be controlled by both a bench pulse generator and the Arduino UNO board. With DC input voltages ranging from 2 to 15 volts, the stimulus circuit controlled by a pulse generator was capable of creating stimuli with peak voltages between 41.8 to 135 volts. With the same input voltages, the stimulus circuit controlled by an Arduino UNO was capable of creating stimuli with peak voltages between 38 to 107 volts. The specific peak voltage necessary for the thumb to twitch varied based on the resistance of the skin, the placement of electrodes, and the type of electrodes used. However, both stimulus circuit controllers were easily able to causing nerves to generate motor action potentials under normal test conditions.

The goal was to have a stimulus that was not painful for the test subject. In most cases, the device was not painful, but caused a mild tingling sensation. However, the device was painful in two cases. The first case was when the stimulus was roughly 135 volts or higher. The second case was when the stimulus burned the skin after several hundred tests.

The goal was to have a stimulus that generated at up to 25 milliamps. The stimulus circuit was capable of generating a maximum of 31.36 milliamps. This current was sufficient for consistently stimulating the median and ulnar nerves to cause motor responses.

The initial goal was to have the stimulus duration be between 1.0 to 1.5 milliseconds. After some more research, the minimum goal was lowered to 0.1 milliseconds. The actual stimulus duration varied from approximately 0.5 milliseconds to 2.5 milliseconds based on the peak stimulus voltage. The duration could easily be increased beyond 2.5 milliseconds, but not decreased below 0.5 milliseconds. This duration was sufficient for consistently stimulating the median and ulnar nerves.

The stimulus waveform had a longer trailing edge than was intended. However, the trailing edge was not reduced because it was not preventing the stimulus from causing motor action potentials. Two of the stimulus waveforms observed by Pereira et al. in commercial devices had long trailing edges as well [20].

The stimulus circuit caused significant noise in the electrical recordings of the arm. Reducing the duration of the stimulus and moving the stimulus circuit away from the bio-amplifier reduced this noise. The noise was reduced to the point where it did not last long enough to interfere with recording nerve action potentials. However, it was never eliminated.

The stimulus circuit unintentionally produced a low DC voltage after it generated the high voltage stimulus peak. However, the stimulus circuit was not changed to remove the DC voltage because the DC

voltage did not harm the test subject or negatively affect the ability of the stimulus to cause action potentials.

Both stainless steel and foam-gel electrodes were effective at stimulating both the median and ulnar nerves. However, after extended use, the stainless steel electrodes caused burns where they contacted the skin. Applying electrolytic gel to the skin and electrodes increased the number of stimulations that could be performed with the stainless electrodes before they caused a burn. However, the electrodes would still eventually cause burns after extended use. The average number of stimulations that the stainless steel electrodes could perform without gel before they burned the skin was not recorded. However, around 1000 stimulations could be performed with gel before they burned the skin.

The custom-made bio-amplifier built from basic components was able to amplify and filter signals. However, its output had more random noise than the output of the bench amplifier. Because of this, the bench amplifier was used in the majority of the later testing. In the end, neither the custom-made bio-amplifier, nor the bench amplifier was able to detect median sensory or motor nerve signals.

A program was used to average multiple recordings together in an attempt to reduce random noise. Averaging recordings together significantly reduced random noise. However, even after averaging no nerve signals were visible.

Isolating the recording device from earth ground was necessary to stop the stimulus from grounding to it. The isolation stage of the custom-made bio-amplifier successfully isolated the test subject from earth ground. The custom-made isolation circuit for the bench amplifier also successfully isolated the test subject. However, it could not be used because it added significant noise to the input of the bench amplifier. Using a large battery to power the bench amplifier isolated the bench amplifier from earth

ground. The input to the bench amplifier had had significantly less noise when this method of isolation was used than when the custom-made isolation circuit was used.

The average twitch response time of a finger when stimulating three quarters of an inch below the wrist was between 8 to 14 milliseconds (Figure 70). The standard deviation between sets of response tests was significant enough to make drawing conclusions difficult. No consistent, significant changes in the response times of either finger were caused by exercising the hand or compressing the wrist. No significant change was seen in the force the thumb exerts while the wrist was being compressed. It seems likely that response times will increase significantly, as the electrodes are placed further from the wrist. Moving both the electrodes slightly off the nerve may also cause response times to increase significantly. However, not enough testing was done to estimate the impact either of these placements will have.

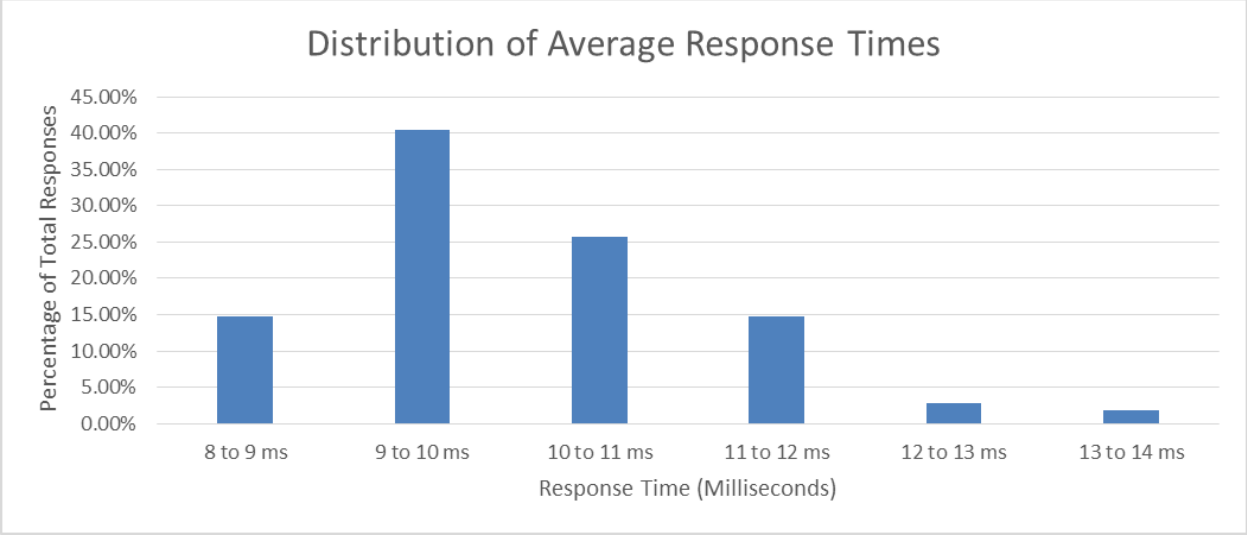

Figure 70: The distribution of average response times based on 109 sets of tests

5. CONCLUSION AND DISCUSSION

5.1 Design Significance

Neither of the two simple devices designed over the course of this research to evaluate nerve health assessed nerve health successfully. However, the stimulus used for both devices was very effective at stimulating motor nerve action potentials. Furthermore, many observations were made during the course of this research that may be used to improve current electronic devices for assessing nerve health or develop new devices.

This research looked in-depth at the electrical circuitry used to stimulate and record nerve action potentials. Many scientific papers about nerve conduction studies and other neurological tests were consulted over the course of this research. Most of these studies were concerned with the application of these devices rather than their design and development. All of these studies used existing medical devices to do their research. Only one study, Pereira et al., modified an existing device using additional electrical circuitry [20]. None of studies designed their own devices from basic components like this research did.

This research lead to the creation and testing of several electronic circuits. Diagrams and discussion of those circuits are presented in this paper and should allow future researcher to reproduce the devices. The bio-amplifier architecture used by this research is not unique or new. However, new information was gained from the tests performed with it. No other research could be found that attempted to use a custom-made device like this for nerve conduction studies. This research could serve as a foundation for future researchers who want to design their own nerve conduction study devices.

The inductor-based stimulus design was not based on any previous research or products. Other nerve conduction devices probably also use inductors to generate their stimuli. However, no documentation could be found to confirm this. This lack of information may be due to the fact these devices are created by private companies. This design gives future researchers a simple way and effective to generate their own stimuli.

The Arduino UNO-based motor response sensing circuit was also not based on any previous research or products. The code that was created during this research for this device is available online for future researchers to use (Appendix: Program 7). This design gives future researchers a simple way to measure the motor responses of digits.

5.2 Future Improvements

The stimulus was effective at stimulating motor nerve action potentials in both the median and ulnar nerves. It can be used by future researchers attempting to measure the twitch response of the thumb or little finger. While the ability of this device to cause sensory nerve action potentials was not verified, it seems very likely that it could cause them. Future research could confirm the ability of this stimulus to cause sensory action potentials by using it with a device that monitors nerves for action potentials.

While the stimulus was only tested on the median and ulnar nerves, it seems likely that it would be able to stimulate other nerves. Future research could test the stimulus on other peripheral nerves. The nerves of the lower leg would be a good target for testing because there should be a noticeable motor response in the toes.

The stimulus was painful when it had a high peak voltage and when it burned the skin. A narrower stimulus peak would likely be less painful and less likely to cause burns. The shortest stimulus used by

this research lasted about 0.5 milliseconds. A higher henry inductor with a lower input voltage may be able to generate a narrower peak. Future research could test this and search for other methods to make the stimulus narrower than 0.5 milliseconds.

Electromagnetic noise from the stimulus was reduced to the point where it would not interfere with recording action potentials. To accomplish this, the stimulus and the bio-amplifier had to be separated by several feet from each other. Future research could search for more practical methods of reducing the electromagnetic noise. Reducing the stimulus width further would likely reduce the electromagnetic noise. In addition, shielding both the stimulus circuit and the bio-amplifier may reduce the electromagnetic noise. Lastly, using shorter cables that are better shielded may reduce the electromagnetic noise.

The custom-made bio-amplifier had more random noise in its output than the bench amplifier. Encasing the bio-amplifier in some form of shielding may reduce this random noise. Future research could attempt to create a more noise-resistant bio-amplifier.

Neither the bio-amplifier nor the bench amplifier was able to observe an action potential. It was originally suspected that there was too much noise in both their outputs. After the bench amplifier was isolated from earth ground by using a battery to power it, its output contained relatively little noise. However, there was still no visible action potentials. Future research could determine why these devices were unable to detect nerve signals.

The testing devices were isolated from earth ground to prevent the stimulus voltage from jumping to them. In the end, the bench amplifier was isolated by powering it with a battery. For the bench amplifier to be fully isolated from earth ground, the oscilloscope that was displaying its output also had to be powered by a battery. The oscilloscope consumed a significant amount of power. The battery used could only power both oscilloscope and the bench amplifier for one hour before it had to be recharged

overnight. This time restriction limited the number of tests that could be done in a day. Because of this limitation, future research could test alternatives to battery-based isolation such as low noise isolation amplifiers or isolation transformers. Alternatively, replacing the bench oscilloscope with a handheld oscilloscope would reduce the power load of the battery significantly. Without having to power the oscilloscope, the battery may last long enough for it to be practical.

The Arduino UNO-based device that measured the motor response of digit was simple and compact. This device worked with a standard personal computer. The device hardware was simpler and cheaper because the computer could be used as its display and used to control it. Because it was so simple, this device could potentially be made into a portable testing device. The development of simpler electronic devices like this could reduce the cost of diagnosis and increase the number of locations able to perform diagnosis.

The device that measured the motor response of a digit made measurements by recording physical movement of that digit. The set-up that the device used to record motor responses was very sensitive to movement and appeared to give accurate results. Alternatively, the measurements could have been made by recording an electromyogram of the muscles of the hand. The Nervepace Electroneurometer assesses nerve heath using an electromyogram [8]. Future research could compare the two methods of sensing motor responses to confirm that their measurements are similar.

The device that measured the motor response of a digit did not detect when the innervating nerve was compressed. However, this does not necessarily mean that it would not detect carpal tunnel syndrome. Carpal tunnel syndrome could have a stronger effect on the twitch response of a digit than compression. Future research could test this device with people affected by carpal tunnel syndrome to see if it can detect the disorder. Future research could also attempt to find a method of nerve compression that accurately simulated carpal tunnel syndrome.

Other factors may have affected the motor response of a digit besides nerve conduction velocity. The muscles being stimulated may have tired after extended testing. The muscle tissue may have become accustomed to contracting and started contracting faster. The resistance of the skin may have decreased because the hand started sweating. The electrolytic gel may have filled small gaps in the skin causing the resistance between the electrodes and the skin to decrease. The electrolytic gel used with the bar and ring electrodes may have dried causing the resistance between the electrodes and the skin to increase. Future research could use a more consistent motor-response testing device to calculate the effect these factors have on response times.

If an electronic nerve testing device was created that was inexpensive and simple to operate, it could be used a self-testing device. The availability of self-testing devices for progressive neuropathies could allow people affected by such conditions to test themselves on a regular basis. This would allow them to monitor whether their condition is worsening over time. The Arduino UNO-based device to measure the twitch response of the digit was relatively simple to use. The most complicated part was the correct placement of the electrodes on the nerve. If the electrodes were not correctly placed, the motor repose of the digit would take significantly longer. A standardized electrode placement location or distance from the digit may reduce error. Future research could create and use standardized electrode placement locations.

Several Matlab programs were written over the course of this research. Information about them is included in the appendix section of this paper. The most significant of these programs is the program to control the Arduino UNO-based device that measured the motor response of digit (Appendix: Program 7). These programs may be useful for future researchers recording signals from the body.

APPENDIX

Code

Code used in this research can be found online at https://gist.github.com/PetSven. Descriptions of the attached programs are included below.

Program 1
File Name: highpassfilter.m
Description: This program calculates the resistor and capacitor values needed to make a high-pass Sallen-Key filter with a given cutoff frequency.

Program 2
File Name: lowpassfilter.m
Description: This program calculates the resistor and capacitor values needed to make a low-pass Sallen-Key filter with a given cutoff frequency.

Program 3
File Name: graph.m
Description: This program graphs CSV files created by exporting a waveform from an oscilloscope.

Program 4
File Name: myfft.m
Description: This program graphs the frequency spectrum and power spectral density of a waveform.

Program 5
File Name: noisefilter.m
Description: This program filters out 60-hertz noise from a waveform.

Program 6
File Name: averagegraph.m
Description: This program averages and then graphs multiple CSV file created by an oscilloscope.

Program 7
File Name: twitch.ino
Description: This program controls the Arduino UNO-based stimulus and twitch sensing device.

REFERENCES

[1] K. Todnem, G. Knudsen, T. Riise, H. Nyland, and J. A. Aarli, “The non-linear relationship between nerve conduction velocity and skin temperature,” *J. Neurol. Neurosurg. Psychiatry*, vol. 52, no. 4, pp. 497–501, Apr. 1989.

[2] R. Kunhimangalam, S. Ovallath, and P. K. Joseph, “Computer aided diagnostic problem solving: Identification of peripheral nerve disorders,” *IRBM*, vol. 34, no. 3, pp. 244–251, Jun. 2013.

[3] C. Burton, L. S. Chesterton, and G. Davenport, “Diagnosing and managing carpal tunnel syndrome in primary care,” *Br. J. Gen. Pract.*, vol. 64, no. 622, pp. 262–263, May 2014.

[4] National Institute of Neurological Disorders and Stroke, “Carpal Tunnel Syndrome Fact Sheet,” 10-May-2017. [Online]. Available: https://www.ninds.nih.gov/Disorders/Patient-Caregiver-Education/Fact-Sheets/Carpal-Tunnel-Syndrome-Fact-Sheet.

[5] Mayo Clinic, “Carpal tunnel syndrome - Symptoms and causes,” 23-Jan-2018. [Online]. Available: http://www.mayoclinic.org/diseases-conditions/carpal-tunnel-syndrome/symptoms-causes/syc-20355603.

[6] I. Atroshi, “Prevalence of Carpal Tunnel Syndrome in a General Population,” *JAMA*, vol. 282, no. 2, p. 153, Jul. 1999.

[7] D. R. Steinberg, R. H. Gelberman, B. Rydevik, and G. Lundborg, “The utility of portable nerve conduction testing for patients with carpal tunnel syndrome: a prospective clinical study,” *J. Hand Surg.*, vol. 17, no. 1, pp. 77–81, Jan. 1992.

[8] W. S. David, V. Chaudhry, A. H. Dubin, and R. W. Shields, “Literature review: Nervepace digital electroneurometer in the diagnosis of carpal tunnel syndrome,” *Muscle Nerve*, vol. 27, no. 3, pp. 378–385, Mar. 2003.

[9] Washington State Department of Labor and Industries, Office of the Medical Director, “Health Technology Assessment Brief: Brevio Nerve Conduction System,” 11-Jun-2007. [Online]. Available: http://www.lni.wa.gov/ClaimsIns/Files/OMD/BrevioAssessment.pdf.

[10] G. Cruccu *et al.*, “EFNS guidelines on neuropathic pain assessment,” *Eur. J. Neurol.*, vol. 11, no. 3, pp. 153–162, Mar. 2004.

[11] G. James and C. Scott, “Vibration testing: A pilot study investigating the intra-tester reliability of the Vibrameter for the Median and Ulnar nerves,” *Man. Ther.*, vol. 17, no. 4, pp. 369–372, Aug. 2012.

[12] E. O’ Conaire, A. Rushton, and C. Wright, “The assessment of vibration sense in the musculoskeletal examination: Moving towards a valid and reliable quantitative approach to vibration testing in clinical practice,” *Man. Ther.*, vol. 16, no. 3, pp. 296–300, Jun. 2011.

[13] R. Parvin, A. N. Nakhostin, N. Soofia, F. Bijan, and H. Scott, “Relationship between Semmes-Weinstein Monofilaments perception Test and sensory nerve conduction studies in Carpal Tunnel Syndrome,” *NeuroRehabilitation*, no. 3, pp. 543–552, 2014.

[14] Y. Son, M. Ha, D. Han, and J. Moon, “Usefulness of the Median Sensory Nerve for the Evaluation of Median Nerve Injuries,” *J. Phys. Ther. Sci.*, vol. 24, no. 11, pp. 1083–1086, 2012.

[15] M. Alemdar, “Effects of gender and age on median and ulnar nerve sensory responses over ring finger,” *J. Electromyogr. Kinesiol.*, vol. 24, no. 1, pp. 52–57, Feb. 2014.

[16] T. M. Ruediger, S. C. Allison, J. M. Moore, and R. S. Wainner, “Reliability, reference values and predictor variables of the ulnar sensory nerve in disease free adults,” *Neurophysiol. Clin. Neurophysiol.*, vol. 44, no. 3, pp. 281–289, Sep. 2014.

[17] M. C. Kiernan, “Effects of temperature on the excitability properties of human motor axons,” *Brain*, vol. 124, no. 4, pp. 816–825, Apr. 2001.

[18] S. J. Oh, S. Hemmi, and Y. Hatanaka, “On-nerve needle nerve conduction study in the sural nerve: A new technique for evaluation of peripheral neuropathy,” *Clin. Neurophysiol.*, vol. 126, no. 9, pp. 1811–1816, Sep. 2015.

[19] W. C. Wiederholt, “Stimulus intensity and site of excitation in human median nerve sensory fibres,” *J. Neurol. Neurosurg. Psychiatry*, vol. 33, no. 4, pp. 438–441, Aug. 1970.

[20] P. Pereira, J. Leote, C. Cabib, J. Casanova-Molla, and J. Valls-Sole, “Stimulus waveform determines the characteristics of sensory nerve action potentials,” *Clin. Neurophysiol.*, vol. 127, no. 3, pp. 1879–1885, Mar. 2016.

[21] I. Aprile, E. Stålberg, P. Tonali, and L. Padua, “Double peak sensory responses at submaximal stimulation,” *Clin. Neurophysiol.*, vol. 114, no. 2, pp. 256–262, Feb. 2003.

[22] A. Wongsarnpigoon, J. P. Woock, and W. M. Grill, “Efficiency Analysis of Waveform Shape for Electrical Excitation of Nerve Fibers,” *IEEE Trans. Neural Syst. Rehabil. Eng.*, vol. 18, no. 3, pp. 319–328, Jun. 2010.

[23] A. Wongsarnpigoon and W. M. Grill, “Energy-efficient waveform shapes for neural stimulation revealed with a genetic algorithm,” *J. Neural Eng.*, vol. 7, no. 4, p. 046009, Aug. 2010.

[24] A. Tamura *et al.*, “Stimulus duration and pain in nerve conduction studies: Stimulus Duration and Pain,” *Muscle Nerve*, vol. 47, no. 1, pp. 12–16, Jan. 2013.

[25] BK Precision, “4050 Series, Dual Channel Function / Arbitrary Waveform Generators,” 08-Jul-2014. [Online]. Available: https://bkpmedia.s3.amazonaws.com/downloads/datasheets/en-us/4050_series_datasheet.pdf.

[26] Keysight Technologies, “33500B Series, Waveform Generators,” 10-Nov-2015. [Online]. Available: http://literature.cdn.keysight.com/litweb/pdf/5991-0692EN.pdf.

[27] J. Rosell, J. Colominas, P. Riu, R. Pallas-Areny, and J. G. Webster, “Skin impedance from 1 Hz to 1 MHz,” *IEEE Trans. Biomed. Eng.*, vol. 35, no. 8, pp. 649–651, Aug. 1988.

[28] Department of Electrical and Computer Engineering, “Lab #2: Bioamplifier Design with Patient Isolation.” 11-Feb-2016.

[29] J. Nashed, K. Calder, R. Trachter, and L. McLean, “The consequences of stimulus intensity on sensory nerve action potentials,” *J. Neurosci. Methods*, vol. 185, no. 1, pp. 108–115, Dec. 2009.

[30] R. M. Buschbacher and N. D. Prahlow, *Manual of nerve conduction studies*. New York, N.Y.: Demos Medical Pub., 2006.

[31] Texas Instruments, “INA12x Precision, Low-Power Instrumentation Amplifiers,” 27-Oct-2016. [Online]. Available: http://www.ti.com/lit/ds/symlink/ina129.pdf.

[32] Vishay, “Standard Carbon Film Leaded Resistors,” 05-Jun-2013. [Online]. Available: https://www.vishay.com/docs/20135/lca.pdf.

[33] “Lead-Lok A7 Solid Gel ECG Electrode : Lead-Lok A7 : Medical Supplies.” [Online]. Available: https://discountcardiology.com/Lead-Lok-A7-Solid-Gel-ECG-Electrode.html. [Accessed: 18-Apr-2018].

[34] “MFI Medical Bar EMG Electrode,” *MFI Medical Equipment, Inc.* [Online]. Available: https://mfimedical.com/products/bar-emg-electrode. [Accessed: 18-Apr-2018].

[35] “MFI Medical Ring EMG Electrodes,” *MFI Medical Equipment, Inc.* [Online]. Available: https://mfimedical.com/products/ring-emg-electrodes. [Accessed: 18-Apr-2018].

[36] Arduino, “analogRead(),” 03-Dec-2017. [Online]. Available: https://www.arduino.cc/reference/en/language/functions/analog-io/analogread/.